N71-13464

UNIVERSITY OF BRADFORD

School of Chemistry

THE FORMATION OF SURFACE FILMS BY ELECTRON BOMBARDMENT

Final report of work carried out during the period
October 1969 - September 1970
at the School of Chemistry,
The University of Bradford

by

Professor M. W. Roberts, Dr. J. R. H. Ross, Mr. J. H. Wood,
Mr. W. J. Murphy and Mr. S. J. Frost

October 1970

FOREWORD

This final report presents the work accomplished by the University of Bradford, Bradford, England, to investigate the mechanism of formation and the properties of thin polymeric films formed from organic monomers in the presence of an electron emitting incandescent filament. The work was performed for TRW Systems Group, Redondo Beach, California, under Subcontract Number CM137, funded under the NASA contract NAS 7-717 entitled "Advanced Spacecraft Valve Technology". The NAS 7-717 programme was undertaken for the purpose of advancing valve technology for liquid propulsion spacecraft engines for the Chief, Liquid Propulsion Technology, Code RPL, Headquarters, National Aeronautics and Space Administration, Washington, D.C. The headquarters Project Manager is Mr. F. Compitello. The NAS 7-717 programme was administered under the technical direction of Mr. L. R. Toth of the Jet Propulsion Laboratory, Pasadena, California.

The TRW Systems Group Programme Manager is Mr. R. J. Salvinski of the Science and Technology Division. Dr. H. T. Mann and Mr. R. L. Hammel of TRW provided technical direction to the University of Bradford on the programme.

Professor M. W. Roberts, B.Sc., Ph.D., D.Sc., F.R.I.C. and Dr. J.R.H. Ross, B.Sc., Ph.D. directed the research. The experimental work was carried out by J. H. Wood, B.Tech., W. J. Murphy, B.Sc., and S. J. Frost, B.Tech., all of whom are graduate students who will subsequently submit the work in fulfilment of the requirements for Ph.D. degrees at the University of Bradford.

ABSTRACT

This report presents the work carried out at the University of Bradford during the period October 1969 to September 1970 to elucidate the mechanism of formation and the properties of thin organic polymeric films prepared by the electron beam polymerisation process. Part I summarises the work reported in the literature on this and related processes and then discusses our earlier progress. Parts 2 to 4 subsequently describe three different fields of study. Part 2 describes work carried out to characterise the reactions occurring in the tungsten emitting filament during the polymerisation process; both W_2C and WC are formed, and changes occur in the apparent thermionic work function of the emitter. Although the thermionic work function of the carburised tungsten is much lower than that of tungsten, it is shown that the average work function is higher. Part 3 describes the characterisation of rhenium as an emitting filament; although rhenium has previously been thought not to form carbides, the present results indicate that a carbide is in fact formed. Part 4 presents the results of studies of the surface properties of thin polymer films prepared under various conditions from perfluorobutene-2; variation of the reaction conditions causes very considerable changes in the surface characteristics. Part 5 suggests further work which should be attempted and Part 6 summarises possible new technology arising from the present programme.

CONTENTS.

1.0 INTRODUCTION AND SUMMARY

1.1. OBJECTIVE.

This final report gives the results of work carried out by the University of Bradford under sub-contract to T.R.W. Systems Group, Redondo Beach, California, as part of the Advanced Spacecraft Valve Technology Programme. The report represents the period October 1969 to September 1970 and represents a continuation of efforts performed during the period 1966 to 1969.[1,2,3] The objectives of the work are to determine and understand the physical and chemical properties of thin polymeric films applied by electron beam techniques to metal substrates. In the earlier stages of the work, it was shown that the polymerisation reaction probably involved the formation of negative ions at the emitting tungsten filament. These ions subsequently polymerise on the substrate; carburisation of the tungsten also occurred. During the present period, it was required to change the chemical structure of the electron emitting filament and to examine its effect on the kinetics of negative ion formation. It was hoped it would be possible to find a more stable emitter. Rhenium was chosen as a possible filament material. It was also required to gain further information on the carburisation of tungsten, but this was subsidiary to the main programme. It has also been shown that films formed from perfluorinated hydrocarbons are relatively inert to chemical attack, and it was shown that considerable insight into the properties of the surface could be obtained by contact angle measurements. These studies have therefore been extended in order to investigate the effect of various polymerisation conditions (such as substrate or filament temperature, monomer flow rate, and electron gun voltages) on the surface characteristics of the polymers so formed, with particular emphasis on their wetting properties.

1.2. HISTORICAL INTRODUCTION.

1.2.1. Early Studies of Polymer Film Formation.

Thin polymeric films have been formed from organic monomers by a variety of techniques, such as (a) electron bombardment, (4 - 17)

(b) ultra violet radiation, (18 - 21)

(c) in glow discharges. (22 - 25)

Table 1.1. Summary of some electron beam polymerisation investigations.

Reference	Monomer(s)	Principal Results
4	Hydrocarbon oils	Mainly hydrogen produced from saturated hydrocarbons, less from unsaturated hydrocarbons.
5	Apiezon greases, picein wax, vacuum cements, silicon greases	Such compounds responsible for polymers in electron microscopes.
6	Diffusion pump oils (hydrocarbons and silicones), vacuum grease, gasket materials, vacuum wax	Similar to ref.(5)
7	Silicone pump oil	Mechanistic study: invokes interaction of electrons with adsorbed layer forming free radicals.
8,9,10,11	DC704	Mechanistic studies and studies of properties of polymers formed. Similar mechanism to ref.(7).
12	MS 704 and MS 200 fluids	Electrical properties
13,14	Butadiene	Mechanism involves interaction of adsorbed molecules with positive species in polymer.
15	Epon 828	Study of use for device technology
16	Epoxy resin	Electrical properties. Stability to thermal cycling
17	Negative photoresist	Effect of electron energy on crosslinking.

Table 1.2. Summary of some ultraviolet polymerisation investigations.

Reference	Monomer(s)	Principal Results
18	Butadiene	Methods of forming suitable patterns described.
19	"	Physical properties discussed.
20	Methylmethacrylate	Polymer properties.
21	Acrylonitrile Methylmethacrylate Styrene Butadiene 2,4-hexadiene Hexachlorobutadiene Tetrafluorethylene	Multiple reflection infra-red analysis of products, and electron diffraction studies.

Table 1.3. Summary of some glow discharge polymerisation investigations.

22	Styrene, methylmethacrylate, benzene, fluorinated hydrocarbons, etc.	Physical properties and chemical constitution of films discussed.
23	CH_3, C_6H_6, C_2H_2, tetracyanoethylene, ferrocene, etc.	Electrical properties.
12	Siloxanes	Electrical properties.
24	Styrene, etc.	Mechanism involving adsorption of monomer proposed.
25	Styrene	Mechanism involves reactions of the radicals formed on the electrodes by electron bombardment.

Table 1.1 summarises some of the work which has been carried out using the electron bombardment technique, and Tables 1.2 and 1.3 show similar details for studies involving ultraviolet and glow discharge polymerisation respectively. In general, the method of formation of the films has been dictated by the vapour pressure of the monomer. If the vapour pressure is greater than about 1 torr, then the discharge tube method has been used; however, the method has the disadvantage that the energy of the particles in the discharge is not uniform and so the properties of the resultant polymer cannot be controlled accurately. Several different mechanisms for the reaction have been proposed.[24,25] Polymerisation by the ultraviolet method is limited to molecules containing double bonds which may be excited by the radiation e.g. such molecules as butadiene[18,19,21] and methylmethacrylate.[20,21] Polymers formed by this method tend to be soft and flexible with properties like those of the bulk polymer; there are also difficulties due to gas-phase polymerisation and deposition on the quartz windows. The electron beam polymerisation method gives the best control of the polymerisation process, as a mono-energetic beam of particles is produced and clearly defined patterns of polymer may be produced by focussing the beam. The disadvantage of the method is that the polymerisation rate is lower, as the monomer pressure is restricted to about 10^{-3} torr. Prior to the present programme, polymers had been formed from vacuum greases,[5,6] diffusion pump oils,[6-12] butadiene,[13,14] epoxy resins,[16] and methyl siloxanes.[12] The mechanism of the reaction was thought to involve either the interaction of electrons with completed polymer which subsequently reacted with further monomer,[13,14] or the interaction of electrons with adsorbed monomer.[7-11]

1.2.2. Adsorption Studies.

Particular attention[8-11] has in the past been paid to polymerisation of the silicon oil, DC704, which most probably has the structure

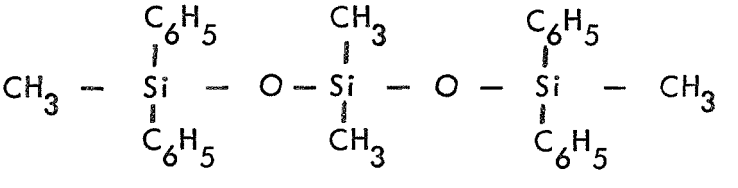

The films produced from this monomer were considered to have potential applications such as anti-cold welding coatings, lubrication, propellant compatability and seal technology.

It was required to examine the kinetics and mechanism of the polymerisation process involving such molecules and to examine the properties of films prepared from various monomers under various conditions.

Initially, it was decided to study the reaction using the less complicated molecule, tetramethylsilane,

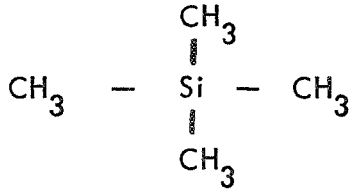

which has a much higher vapour pressure and which could therefore be handled quantitatively. The central silicon atom of $Si(CH_3)_4$ has a similar type of bonding to that of the central silicon atom of DC 704 and also the products of any reaction would be much simpler than from DC 704 so that the kinetics and stoichiometry of the reaction were amenable to mass-spectrometric analysis.

As the bonding of the polymer to the substrate, and hence its adhesion, depend on the nature of the interaction of the monomer with the surface, and as no previous studies of the adsorption of silicon compounds by metal surfaces had been carried out, the chemisorption of $Si(CH_3)_4$ by atomically clean tungsten and iron surfaces was examined initially.[1] The results were obtained employing ultrahigh vacuum techniques and using evaporated metal films of the two metals. It was found that both metals caused considerable dissociation of the $Si(CH_3)_4$ molecule, the extent of the reaction increasing with increasing temperatures, and being more marked for tungsten. The product gases include methane, which indicated that carbon-silicon bonds were cleaved during the chemisorption process; this result is in contrast to that obtained for the adsorption of neopentane ($C(CH_3)_4$) by tungsten films where there was evidence for only very limited carbon-carbon bond cleavage. Hence, it was suggested that tungsten would be a better substrate than iron for thin polymeric films, as the adhesion would be greater.

1.2.3. Proposed Mechanism of the Polymerisation Process.

When an electron emitting filament was introduced into the reaction vessel used in the adsorption study, the rate of reaction was found[1] to be close to the rate at which

molecules from the gas phase collide with the filament, and it was implied that the reaction at the filament is the rate determining step. In a parallel investigation in which polymers were formed for chemical testing in a flow system[2] (see below), it was observed that the emission current from the filament was a function of the monomer pressure and of the filament temperature. It was suggested[2] that the reactive species might be negative ions formed at the cathode surface, and that these ions subsequently polymerise at the substrate. To test this hypothesis, a magnetron was constructed; this could separate the contribution of electrons and negative ions to the total emission current. Negative ions were indeed observed, and the negative ion current was found to be directly proportional to the pressure of monomer for several molecules ($Si(CH_3)_4$, $C(CH_3)_4$, and butadiene). The temperature dependence of the negative ion current was also investigated for these monomers.[3]

1.2.4. Stoichiometry of the Polymerisation Reaction.

A mass-spectrometric study[2,3] of the polymerisation process using $Si(CH_3)_4$ as a monomer indicated that the nature of the reaction depends on the applied voltage. Without a voltage, the reaction corresponds to carbiding and siliciding of the tungsten emitter, all the hydrogen of the $Si(CH_3)_4$ appears in the gas phase as either molecular hydrogen or as methane. When a voltage is applied, the stoichiometry of the reaction changes once a certain critical voltage is reached, at which voltage, the rate of the reaction increases considerably. The stoichiometry was now assumed to correspond to that of a combination of the formation of negative ions and the subsequent polymerisation reaction; much of the hydrogen from the $Si(CH_3)_4$ is incorporated in the polymer.

1.2.5. Mechanism of Negative Ion Formation.

The voltage at which negative ions start to form was found[3] to depend on the separation of the electron emitting filament from the substrate, and also on the monomer pressure. It was shown that the negative ions are formed by field desorption of species formed from $Si(CH_3)_4$ on the surface of the emitting filament. The nature of the ions and the mechanism of their reaction with the substrate and the growing polymer has not yet been elucidated; it is possible that the negative ion formed is $Si(CH_3)_3^-$.

1.2.6. Reactions of the Filament Material.

The emission characteristics of the tungsten emitter were found to change due to carbiding, during the polymerisation reaction;[3] the nature and extent of the change were dependent on whether or not a field was applied. The reaction was examined in detail using neopentane ($C(CH_3)_4$) and a tungsten filament; the changes in resistance at both room temperature and reaction temperature were noted in addition to obtaining the vacuum emission characteristics. This work has been continued, using a different method of work function determination (the Kelvin method) and the results compared with the results from thermionic emission which have been examined in greater detail. These results are discussed in Part 2 of this report.

As the composition of the emitting filament, and hence its work function, changes with time, depending on the reaction conditions, it was found that the kinetics of the reaction could be studied only semi-quantitatively. In particular, it was not possible to examine the kinetics of the reaction at and around the critical voltage as a function of applied voltage, as the nature of the surface depended largely on the time for which any voltage was applied. Hence, it was decided that an attempt should be made to find a filament material which did not form carbides. It has often been stated that rhenium does not form a carbide,[26] and indeed, it is for this reason that rhenium is frequently used as a filament material in mass-spectrometers, as much greater stability of emission is claimed with rhenium than with tungsten. Part 3 of this report therefore describes results obtained using rhenium filaments; it has been shown that rhenium probably does form a carbide, but that once an initial activation procedure has been carried out, stable emission characteristics are achieved.

1.2.7. Chemical stability of polymer films.

Chemical tests were carried out on polymers formed on tungsten and nickel from a series of monomers.[3] There was some evidence that films formed from perfluorinated monomers had considerable chemical stability and gave protection from chemical attack to the underlying metal. It was therefore desirable to investigate further the properties of such polymers, including chemical, mechanical and surface properties, the last of these being

investigated in some detail (see 1.2.8. below). The films formed were insoluble in common solvents (see below) and were adherent to the underlying substrate material. A more quantitative approach to the determination of the chemical and mechanical properties of the thin polymeric films is clearly desirable. This might be achieved by forming thick films which could be tested by conventional quantitative methods.

1.2.8. Surface Properties of Thin Polymer Films.

The use of contact angle measurements[27] to determine the surface properties of thin polymeric films has been developed. By measuring the angle of contact, θ, (see fig.1.1)

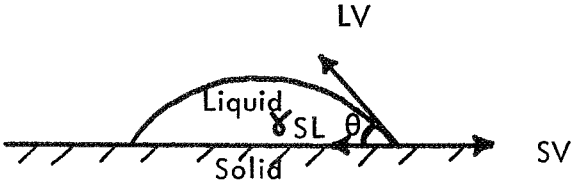

Figure 1.1.

made by drops of pure liquids whose surface tensions γ_{LV} are known, a plot such as that in figure 1.2. may be constructed. The value of γ_{LV} obtained when $\cos\theta = 1$ ($\theta = 0$)

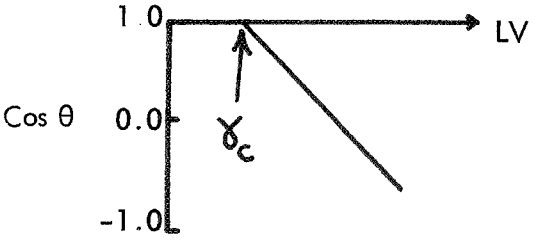

Figure 1.2.

is denoted as γ_c. This has been shown in a series of studies by Zisman and co-workers (see reference 27) to be characteristic of the surface being studied. The lower the value γ_c, the lower is the surface energy of the solid and the less likely is the solid to be wetted by a liquid. It was shown[3] that the technique was applicable to thin films prepared from perfluorobutene-2 on tungsten substrates; the values of critical surface tension were higher than that of bulk teflon, probably due to cross-linking in the polymer, and they were found to vary with preparation conditions. It was also shown that when drops of solutions of methanol or butanol in water were used instead of pure liquids, different values of γ_c were

found, although Bernett and Zisman[28] had shown that solutions and pure liquids gave identical results on polythene and teflon. It was inferred that, contrary to general belief, the alcohol molecules were adsorbed on the polymer surface and that the critical surface tension obtained reflected the adsorbed layer rather than the clean surface. It was shown that the plots of cos θ vs γ_{LV} obtained could be converted into adsorption isotherms relating the number of molecules adsorbed to the solution concentration. The nature of the isotherm was shown to depend on the preparation conditions of the polymer and to give valuable additional information as to the nature of the surface. The general applicability and the reproducibility of the method was checked using bulk samples of polystyrene and polymethylmethacrylate.

Section 4 of this final report discusses the results of an extension of the previous work to a systematic study of the wetting characteristics of the polymers as a function of preparation conditions. These include monomer flux, filament temperature, electron gun characteristics, nature of the substrate, and substrate temperature. It also presents a slight modification of the theory of the method (an assumption made previously has been shown to be unjustified). This theory has been shown, by the use of adsorption techniques, to hold for several systems and the results of this work are presented.

1.3. PROGRAMME PLAN.

1.3.1. Carburisation of tungsten.

This part of the programme was to be concerned with a systematic study of the carburisation of tungsten using resistance and work function methods. A comparison of the various methods of work function determination was also carried out.

1.3.2. Investigation of additional filament materials.

Rhenium was to be investigated as a possible material for the emitting filament. Its behaviour in a hydrocarbon (neopentane) was to be examined and its suitability as a stable emitter assessed.

1.3.3. Wetting Study.

A more detailed evaluation of the theory of the method using bulk conventional polymers was required, together with a systematic investigation of the surface properties of thin polymeric films prepared from perfluorobutene-2 as a function of preparation conditions.

1.4. SUMMARY.

Work carried out by the University of Bradford has shown that under certain conditions the formation of thin polymeric films by the electron beam technique involves reaction of monomer at the electron emitting filament with formation of negative ions and these subsequently polymerise at the substrate. The monomer/emitter reaction has been investigated in some detail, using both tungsten and rhenium filaments. The former metal combines with some of the carbon of the monomer to form carbides (WC and W_2C) and the work function of the resultant surface is largely determined by the reaction conditions (see Part 2). Rhenium has been thought to form only solid solutions with carbon; however, the present study shows that this may not be the case, as under certain conditions during the polymerisation reaction a low work function surface is formed which would not be possible if only solid solutions were formed. A stable emitting surface is formed after a period of reaction, and this could be used satisfactorily for accurate kinetic investigations, which were not possible using a tungsten emitter. The initial stage of the carburisation of rhenium has been examined in some detail using resistance measurements in conjunction with emission measurements, both in vacuum and in the presence of neo-pentane (see part 3.)

It has been shown (see part 4) that the measurement of contact angles of drops of dilute aqueous solutions of organic molecules on the surface of the thin polymer films gives useful information on the nature of the polymer surface. The surface properties of the polymers formed are extremely dependent on the preparation conditions. The theory of the method has been examined in detail using bulk polystyrene and polymethylmethacrylate to verify that the basic assumption involving adsorption of the organic molecule is tenable. The latter results have repercussions in the fields of colloid chemistry and detergency.

It has thus been shown that the reaction of the monomer molecule at the electron emitting

filament is of importance in the polymerisation process and that the properties of the resultant polymer depend on the reaction conditions. By suitable choice of monomer, emitting filament material, and reaction conditions, it is possible, with suitable fundamental information for various monomer/filament combinations, to form extremely reproducible thin polymeric films with any required properties. It should also be possible to predict the properties of films formed with untested combinations.

Contributions have also been made to the basic knowledge of the effect of applied field on reactions at incandescent surfaces and of the solid-state reactions of the filament materials, and to the theory of adsorption from solution by low energy surfaces. Possible new technology suggested by the work, in addition to the applicability of the thin films, includes a negative ion source of high sensitivity for mass-spectrometry, a potentially useful high temperature material (rhenium carbide), and the production of new types of detergents and surface agents which would utilize the phenomenon of adsorption from solution by low energy solids (see Part 6.)

REFERENCES

1. M. W. Roberts and J. R. H Ross, Final Report to T.R.W. Systems, October 1967.
2. M. W. Roberts, J. R H. Ross and J. H. Wood, Final Report to T.R.W. Systems, October 1968.
3. M. W. Roberts, J. R. H. Ross, J. H. Wood and W. J. Murphy, Final Report to T.R.W. Systems, October 1969.
4. C. S Schoepfle and L. H. Connell, Ind. Eng. Chem., 21, 529, (1929).
5. K. M. Poole, Proc. Phys. Soc., B66, 542, (1953).
6. A. E. Ennos, Brit. J. Appl. Phys., 5, 27, (1954).
7. J. A. Buck and K. Shoulders, Proc. Eastern Joint Computer Conference, Philadelphia 1958.
8. R. W. Christy, J. Appl. Phys., 31, 1680, (1960).
9. H. T. Mann, Electrochemical Technology, 1, 287, (1963).
10. H. T. Mann, J. Appl. Phys., 35, 2173, (1964).
11. R. W Christy, J. Appl. Phys., 35, 2179, (1964).
12. G. W. Hill, Microelectronics and Reliability, 4, 109, (1955).
13. I. Haller and P. White, J. Phys. Chem., 67, 1784, (1963).
14. P. White, J. Phys. Chem., 67, 2493, (1963).
15. H. L. Caswell and Y. Budo, Solid State Electronics, 8, 479, (1965).
16. A. E. Brenntmann and L. V. Gregor, J. Electrochem. Soc., 112, 1194, (1965).
17. B. Broyde, J. Electrochem. Soc., 116, 1241, (1969).
18. P. White, Electronics Reliability and Microminiaturisation, 2, 161, (1963).
19. P. White, Electrochemical Technology, 4, 468, (1966).
20. L. V. McGregor and H. L. McGee, Proc. Annual Electron Beam Symposium, Boston, 1963, p.211.
21. A. N. Wright, Nature, 215, 953, (1967).
22. J. Goodman, J. Polymer Science, 44, 551, (1960).
23. A. Bradley and J. P. Hammes, J. Electrochem. Soc., 110, 15, (1963).
24. T. Williams and M. W Hayes, Nature, 209, 769, (1966).
25. A. R. Denaro, P. A. Owens, and A. Crawshaw, European Polymer Journal, 4, 93, (1968).
26. J. E. Hughes, J. Less Common Metals, 1, 377, (1959).
27. W. A Zisman, Advances in Chemistry Series, 43, 1, (1964). (American Chem.Soc.)
28. M. K. Bernett and W. A. Zisman, J. Chem. Phys., 63, 1241, (1959).

2.0. STUDY OF THE CARBURISATION OF TUNGSTEN

2.1. INTRODUCTION.

In the last final report,[1] it was shown that the carburisation behaviour of the emitting tungsten filaments used in previous work depended on the reaction conditions. When carburisation was carried out without an applied field, the predominant product was W_2C, and with an applied field, the main product was WC. The apparent work function of the surface during carbiding without a field, determined from the thermionic measurements, varied from 5.4eV to a value of about 2eV. The pre-exponential factor for the Richardson equation was found to decrease as the work function decreased. A low work function was also obtained for a filament carburised with a field, but these results were not described in detail.

The surface of a polycrystalline metal is composed of patches which are the result of the orientation of crystallites in the bulk of the metal exposing different crystallographic directions at the surface. If a patch has a low work function relative to its neighbours, the emission current given by the Richardson equation will be much higher. The emission current will be directly proportional to the area of the patches. The effect of the low work function is to bias the apparent work function (ϕ^{**}) of the emitter away from the average value and towards that of the low work function patches. It is therefore possible to measure two work functions for a polycrystalline surface, the first ($\bar{\phi}$) being the simple geometric average and the second (ϕ^{**}) being a much more complex function depending on the arrangement of the planes. The difference between $\bar{\phi}$ and ϕ^{**} is determined by the work function and area distributions of the patches. For example, on a polycrystalline tungsten surface, there is a narrow distribution of work functions and so the values determined by the Kelvin and Richardson methods (see below) are similar. In other cases, such as with oxide cathodes, there is a wide range of patches with different work functions, and so $\bar{\phi}$ and ϕ^{**} differ considerably.

This part of the present report therefore presents further data concerning the carburisation of tungsten filaments and describes experiments in which the two work functions $\bar{\phi}$ and ϕ^{**} were determined. Conclusions are reached concerning the nature of the carbides formed using neopentane, tetramethylsilane, and butadiene.

2.2. EXPERIMENTAL.

The apparatus used for the determination of ϕ^{**} and for the study of the carburisation reaction using resistance measurements was described in earlier reports.[1,2] It was a continuously pumped ultra-high vacuum system constructed from pyrex glass, operated with oil diffusion pumps. Hydrocarbon gases were leaked into the system at a known rate to give steady pressures in the range 10^{-4} to 10^{-2} torr. The filament, several cm. of 0.1 mm pure tungsten wire, was mounted in a magnetron cell, used to determine the negative ion emission characteristics described in a previous report.[1] This cell was also used for the vacuum emission measurements involved in the determination of ϕ^{**} at various stages of carbiding. An auxilliary pyrex vessel was used for temperature measurement (optical pyrometry) and this used an equivalent filament not surrounded by an anode; the most accurate measurements were obtained when an optically flat window was included in the cell.

The geometric average value of work function ($\bar{\phi}$) was determined using the vibrating capacitor technique due to Kelvin. The method is a comparative one and the difference of work functions between two flat parallel metal plates is found by vibrating one with respect to the other in a direction normal to both surfaces. An A.C. signal is produced and the contact potential between the two metals ($\bar{\phi}_1 - \bar{\phi}_2$) can be nulled out using an external DC voltage supply, as shown by the disappearance of the signal. Using modern methods of AC detection, the sensitivity of the method can be extremely high. The system used employs phase sensitive detection, which reduces the first harmonic and external A.C. interference to very low levels. The vacuum system utilised was also a flow system, but mercury diffusion pumps were used. In this case, the tungsten was in the form of a ribbon, and the reference electrode was a plane gold plate which could be rotated away from the tungsten during outgassing and carburisation. Gold does not

chemisorb most of the common gases found in ultra-high vacuum systems and so repeated outgassing is not required, as would be the case if some other metal were used as the reference electrode. In mercury pumped systems, gold has a different work function to that in clean systems, such as with oil pumps, but this work function is relatively stable for a given reference plate. The value of the reference work function was determined by comparing it with a well outgassed tungsten ribbon (heated for prolonged periods at 2100K) whose work function was assumed equal to the literature value of 4.55 eV.

Resistance measurements were in most cases made in the magnetron cell. Cold resistances were measured with a conventional Wheatstone Bridge circuit. The filament was cooled from the reaction temperature before each measurement; in experiments of this type, the time of reaction corresponds only to the time at reaction temperature. Hot resistance measurements were made in a slightly different fashion. The Wheatstone Bridge was operated with the higher currents needed to heat the filament; the bridge was balanced initially and then hydrocarbon was admitted to the flow system. The e.m.f. produced at the detector terminals was recorded as a function of time; this was shown to be proportional to the resistance change, ΔR, the proportionality constant being dependent on the initial value of the resistance.

2.3. RESULTS AND DISCUSSION.

2.3.1. Hot Resistance Measurements.

2.3.1.1. Reaction with a field.

Figures 2.1 to 2.3 show the results obtained for the change in hot resistance of a tungsten filament at an initial temperature of 2160K with +30V on the grids and +60V on the anode (w.r.t. the filament) for neopentane, tetramethylsilane, and butadiene. Also shown are the total emission currents as a function of time.

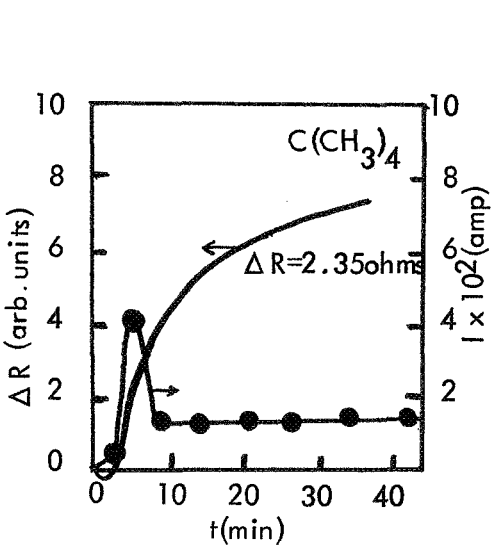

Figure 2.1

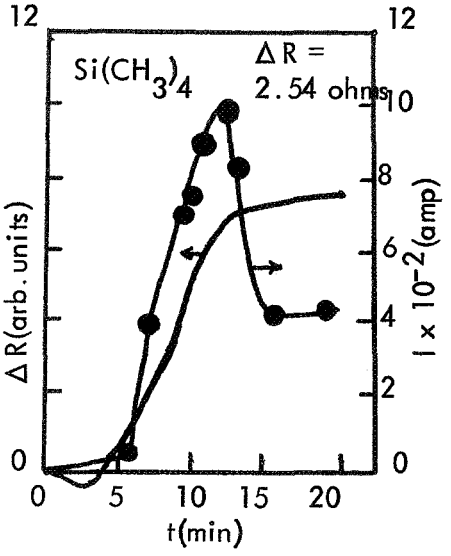

Figure 2.2

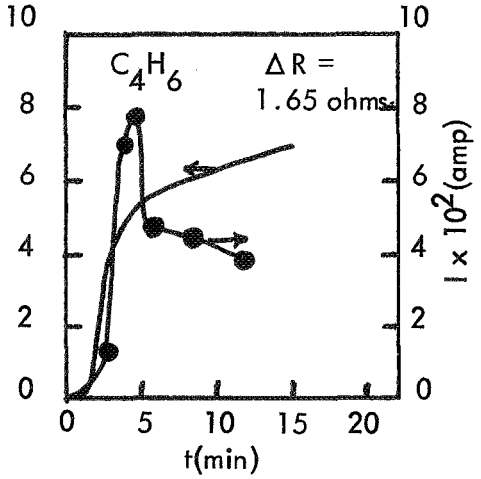

Figure 2.3

Figures 2.1 - 2.3. Hot resistance changes and emission for reaction with a field. (T_f = 2160K, P ≙ 10^{-3} torr)

2.3.1.2. Reaction without a field.

Figures 2.4 to 2.6 show the hot resistance changes as a function of time without an applied field at the same temperature.

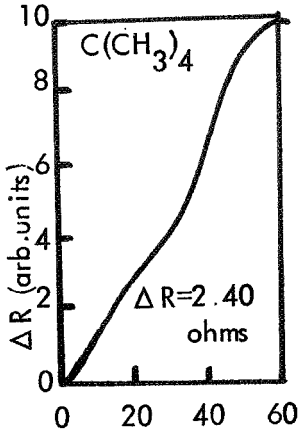

Figure 2.4

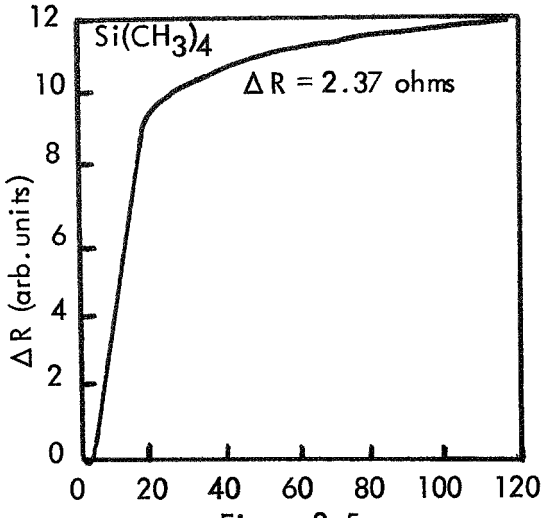

Figure 2.5

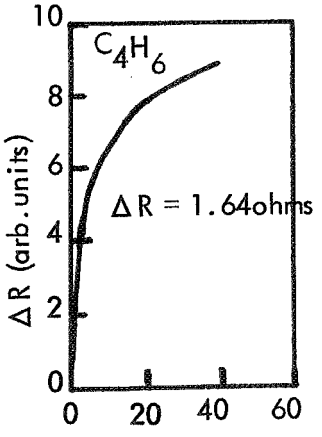

Figure 2.6

Figures 2.4 - 2.6. Hot resistance changes for reaction without a field.
(T_f = 2160K, P $\triangleq 10^{-3}$ torr)

2.3.2. Cold Resistance Changes (Neopentane and Tetramethylsilane).

Only with neopentane and tetramethylsilane was it possible to measure cold resistance changes as a function of time. The results for neopentane without (line 1) and with a field (line 2) are shown in figure 2.7. Figure 2.8 shows similar results for tetramethylsilane without a field.

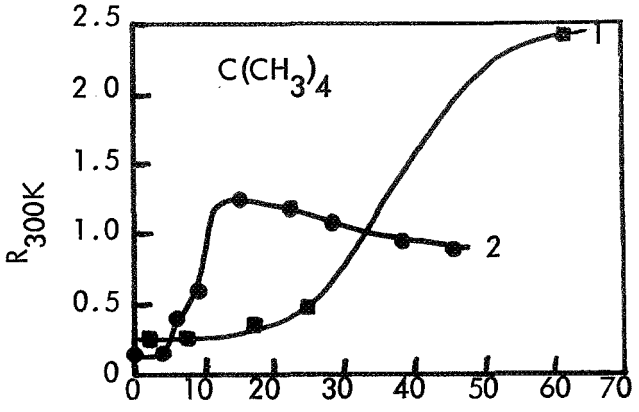

Figure 2.7 Cold resistance changes without (1) and with a field (2)

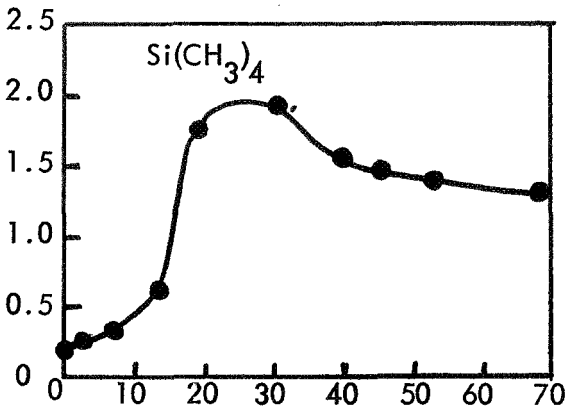

Figure 2.8 Cold resistance change without a field

2.3.3. Effect of cooling the filament during carburisation with butadiene.

Figure 2.9 shows the results of an experiment in which the hot resistance of a tungsten filament was measured during carburisation at 2150K without a field. The reaction was interrupted at point A by cooling the filament to room temperature, when, on raising the temperature again, the hot resistance followed the lower line instead of rising to point B before the rate of change of ΔR decreased. Hence, cooling the filament appears to cause

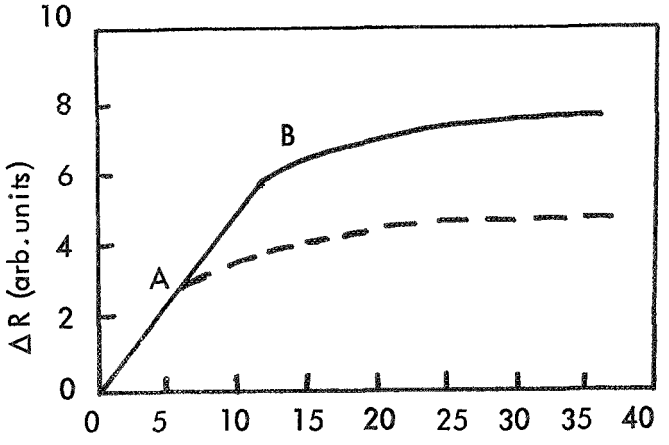

Figure 2.9 Effect of cooling the filament on hot resistance changes (reaction without a field)

a change to occur in the nature of the carburisation reaction, probably involving the formation of WC instead of W_2C (see below); this is probably due to WC being favoured in the surface region at some intermediate temperature, and once it is formed, it affects the rate of reaction in such a way that WC formation is favoured at the upper temperature.

2.3.4. Nature of the carburisation reactions.

Table 2.1 shows the change in hot resistance (ΔR_{2160K}) and the values of the cold resistance (R_{300K}) of the filaments after carbiding with a field for about thirty minutes (the end of the run for figures 2.1 to 2.3) and table 2.2 shows similar values for carbiding without a field (figures 2.4 to 2.6)

Table 2.1. Reaction with a field

	Neopentane	Tetramethylsilane	Butadiene
ΔR_{2160K} (ohms)	2.35	2.54	1.65
R_{300K} (ohms)	1.10	-	-

Table 2.2. Reaction without a field

	Neopentane	Tetramethylsilane	Butadiene
ΔR_{2160K} (ohms)	2.40	2.37	1.64
R_{300K} (ohms)	2.43	0.83	0.71

If it is assumed that the resistance change observed is due to the formation of solely W_2C, these resistance changes can be converted into volume fractions (x) of W_2C, using resistivity data for pure tungsten[3] and W_2C[4] (see reference 5). Tables 2.3 and 2.4 show the resultant figures for reaction with and without a field.

Table 2.3. Volume fractions, x, of W_2C (assuming no WC formation) calculated from tables 2.1 and 2.2 for reaction with a field.

	Neopentane	Tetramethylsilane	Butadiene
x_{2160K}	0.98	1.05	0.68
x_{300K}	0.31	-	-

Table 2.4. Volume fractions, x, of W_2C calculated from tables 2.1 and 2.2 for reaction without a field.

	Neopentane	Tetramethylsilane	Butadiene
x_{2160K}	0.99	0.98	0.68
x_{300K}	0.76	0.22	0.19

If W_2C is the only carbide formed, then the values of x_{2160K} should be the same as the value of x_{300K}. This is not the case: table 2.5 shows the values of the ratio of x_{2160K} / x_{300K} for each case.

Table 2.5. The ratio x_{2160K} / x_{300K} for carburisation of tungsten at 2160K with and without a field, assuming only W_2C formed.

	Neopentane	Tetramethylsilane	Butadiene
With a field	3.16	-	-
Without a field	1.3	4.45	3.58

Only for neopentane without a field is the value of $\frac{x_{2160K}}{x_{300K}}$ approximately unity. Hence it is assumed that only in this case is the product almost entirely W_2C. In the other cases, it is probable that formation of WC occurs almost simultaneously with the formation of W_2C. For example, comparing figures 2.1 and 2.7 (line 2), which

represent hot and cold resistance changes during carburisation with neopentane with an applied field, it is found that the hot resistance rises at first rapidly and then more slowly, whereas the cold resistance rises to Point C and then falls. Hence, up to point C, it is probable that W_2C is the main product, whereas after point C, WC begins to form at an appreciable rate. Similar considerations apply to tetramethylsilane without a field. As mentioned above, the variation of the cold resistance change with time for butadiene could not be determined.

It is known that the resistivity of WC at 2160K is similar to that of W_2C, and that the room temperature resistivity of WC is lower than that of W_2C.[6] Tabulated data are not however available for WC. It has been shown in the present work that this trend is the case (section 2.3.5) and the temperature coefficient of resistivity has been determined. The similarity of resistivities of W_2C and WC at 2160K allows the value of x_{2160K} to be used to indicate the extent of W_2C or WC formation. For both neopentane and tetramethylsilane (tables 2.3 and 2.4) the value is approximately one, showing that both with and without a field, the tungsten is almost completely carbided. The values of the ratio $\frac{x_{2160K}}{x_{300K}}$ for neopentane indicate that much more WC is formed with a field than without, indicating that reaction with a field is more rapid than that without. With tetramethylsilane, where the cold resistances with a field were not examined, the rates of change of hot resistance with and without a field were similar, indicating similar rates of reaction, probably simultaneous formation of W_2C and WC. With butadiene, the rates were again similar with and without a field but much slower than with the other molecules; the filament therefore probably contained considerable quantities of unconverted tungsten as well as W_2C and WC.

2.3.5. Temperature coefficient of resistance for carbided filaments.

Figure 2.10 shows the resistivity/temperature characteristics for (A) tungsten[3] (B) W_2C[4], and (C) WC (see below.) The WC filament was obtained experimentally by carburising a tungsten filament, maintained at an initial temperature of about 2000K for about 14 hours in butadiene at 1×10^{-3} torr. The final cold resistance, after allowance for the resistance of the leads etc. was 0.43 ohms, which is consistent with what is known of WC i.e. the room temperature resistivity is about 2.5 times that of tungsten.

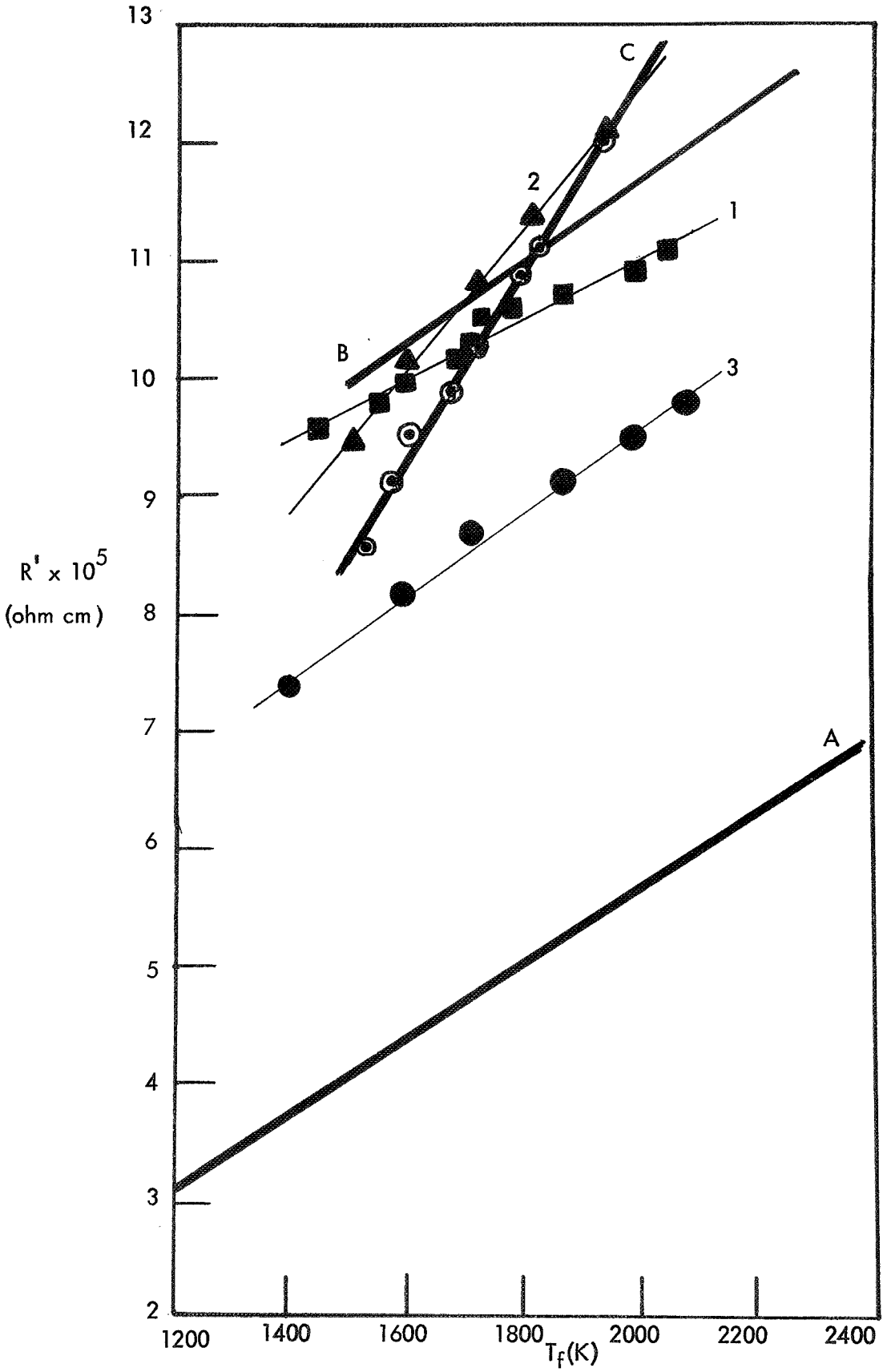

Figure 2.10. Resistivity of filaments as a function of time. A, tungsten; B, W_2C; C, WC; filaments carburised for ~60 minutes at ~2160K in $C(CH_3)_4$ (1), $Si(CH_3)_4$ (2) and C_4H_6 (3).

This filament was then used to obtain line (C) in figure 2.10, using an optical pyrometer for temperature measurement. The resistivity of WC, $R^1_{(WC)}$ between 1500 and 2000K is given by equation 2.1:

$$R^1_{(WC)} = 8.2 \times 10^{-7} T - 3.8 \times 10^{-4} \text{ohm.cm.} \quad \ldots\ldots\ldots (2.1)$$

The temperature/resistivity measurements were then repeated on filaments carburised without a field for shorter periods (the experiments reported in table 2.2). The results are shown in figure 2.10, lines 1, 2 and 3, which correspond to neopentane, tetramethylsilane, and butadiene respectively. Line 1 is similar in shape to line B (W_2C) and so neopentane gives a composition close to W_2C with some unreacted tungsten. Line 2 shows that the filament reacted in tetramethylsilane is almost wholly composed of carbide, being probably a mixture of W_2C and WC. With butadiene (line 3), the proportion of tungsten is very much higher. These conclusions are completely in agreement with the conclusions reached above.

2.3.6. The onset of WC formation.

If, as suggested, the maximum in the cold resistance against time plots (figs. 2.7 and 2.8) is indicative of the commencement of WC formation, certain conclusions can be reached concerning this process. In figures 2.7 and 2.8, the rate of formation of W_2C prior to the maximum is in the order neopentane (with field) $>$ tetramethylsilane (without field) $>$ neopentane (without field), and the value of the maximum resistance is in the opposite order. Hence, it may be concluded that the greater is the rate of carburisation, the sooner does WC start to form; i.e. diffusion of carbon into the bulk must become rate determining, at which stage WC starts to form at the surface and the rate of reaction slows down considerably. The results of figure 2.9 were explained in a similar way (see section 2.3.3.).

If the rate of supply of carbon is important in determining the magnitude of the maximum of the cold resistance plots or of the knee in the hot resistance plots, then the variation of gas pressure may cause a change in the shape of the plots. Figure 2.11 shows three hot resistance plots for different butadiene pressures. The pressure for line 1 was greater than

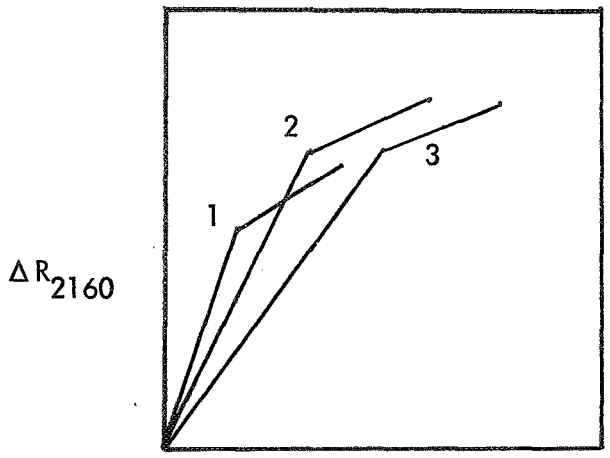

Figure 2.11. Hot resistance changes during carburisation at different pressures of C_4H_6 ($P_1 > P_2 > P_3$)

for line 2 than for line 3. The rate of carbide formation increases with increasing pressure but the knee of the curve falls with increasing rate of reaction, which is in agreement with the conclusions reached above.

2.3.7. Emission during carburisation.

Figures 2.1 to 2.3 also showed the total emission current in the presence of the carbiding molecules (i.e. the current is composed of electrons and negative ions). The emission with each gas rose to a maximum during that time when W_2C formation has been inferred and then fell during the formation of WC. The latter fall has been shown to be due to the change in resistance of the filament and hence the carburisation temperature rather than to a change in the work function of the filament, as would otherwise appear to be the cause. However, such a change in emission current is a good indication that at least a bulk phase change has occurred and the surface is now probably composed of WC (see section 2.3.8.2. below).

2.3.8. Thermionic Work Functions of Carburised Filaments.

2.3.8.1. Work Functions after carburisation.

The determination of the work functions of the carburised filaments was complicated by the fact that the temperature/heating current calibrations to be used were dependent on the nature of the material present i.e. on whether the material comprised mainly tungsten

or W_2C or WC. It was shown[5] that the temperature heating current characteristics of tungsten and WC were similar and quite different to that of W_2C. Hence, in the following table (table 2.6) the work functions obtained assuming both tungsten and W_2C temperatures are given; the more likely value is underlined in those cases when one or other type of carbide is most likely.

Table 2.6 gives the results for the determination of $\emptyset^{**}$ after reaction with a field, as shown in figures 2.1 to 2.3. The filaments and anode were outgassed before each determination.

Table 2.6. Values of $\emptyset^{**}$ (eV) after reaction with various molecules in the presence of a field.

Filament Composition Assumed	Neopentane	Tetramethylsilane	Butadiene
W or WC	1.67	<u>2.49</u>	2.35
W_2C	<u>2.49</u>	3.43	3.6

From these results it would appear that the average thermionic work function of a carburised tungsten surface after reaction with a hydrocarbon gas was about 2.5 eV. This probably corresponds to a surface composed largely of WC, even though the bulk composition may still involve some W_2C and tungsten. A similar value of $\emptyset^{**}$ was obtained for a filament carburised in neopentane with intermittent application of a field.

2.3.8.2. Work functions with Incremental Carburisation of a Tungsten Filament in Neopentane without a Field.

Figures 2.12 to 2.14 show the results of an experiment in which a tungsten filament was carburised at ~2160K without a field in neopentane. We have inferred above that this system forms first W_2C and then WC. Figure 2.12 shows hot resistance data obtained

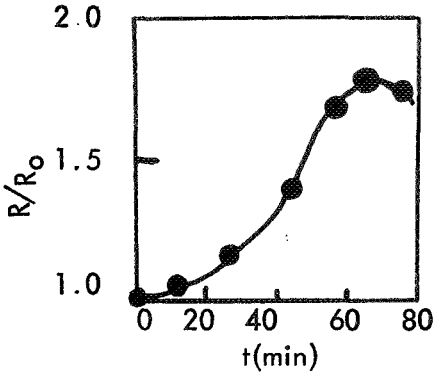

Figure 2.12

Fractional Resistance Change of Filament carburised at 2160K (R = resistance at 1750K & R_o = initial resistance at 1750K.)

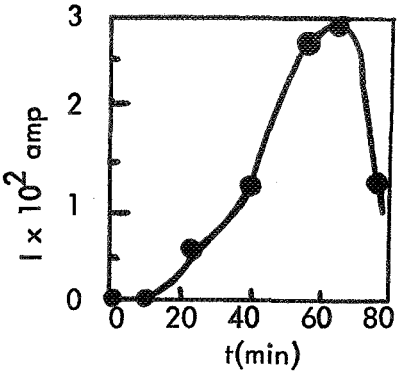

Figure 2.13

Emission Current in vacuum at 1750K as a function of reaction time.

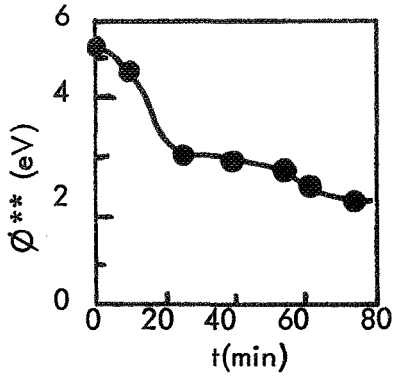

Figure 2.14

Thermionic work function (Ø**) of filament carburised for various times.

at ~1750K, compared with 2160K previously shown, figures 2.1 - 2.6. At this temperature, the resistivity of W_2C and WC differ sufficiently for the hot resistance to drop when WC formation begins to occur. At this point, assuming only W_2C formation, it was calculated that the filament contained 94% W_2C. Figure 2.13 shows the emission current in vacuo at ~1750K as a function of reaction time; the emission rises to a maximum when W_2C formation is complete and then falls when WC formation occurs. Figure 2.14 shows the work function computed from Richardson plots at each stage of carbiding. It falls gradually to a value of about 2.5eV during the formation of W_2C and falls further when WC is formed. Table 2.7 summarises this data and also gives the calculated pre-exponential factor (in $A.K^{-2}cm^{-2}$) for each point.

Table 2.7. Work function (Ø**) and pre-exponential factor (A**) for a tungsten filament at various stages of carburisation in neopentane at 2160K.

Time (min)	0	7	27	42	56	63	77
Ø** (eV)	5.22	4.59	3.10	3.01	2.80	2.47	2.2
A** (Amp.$K^{-2}cm^{-2}$)	$7.2\times10^{+4}$	$1.2\times10^{+5}$	145	46.8	9.12	1.48	7.9×10^{-2}

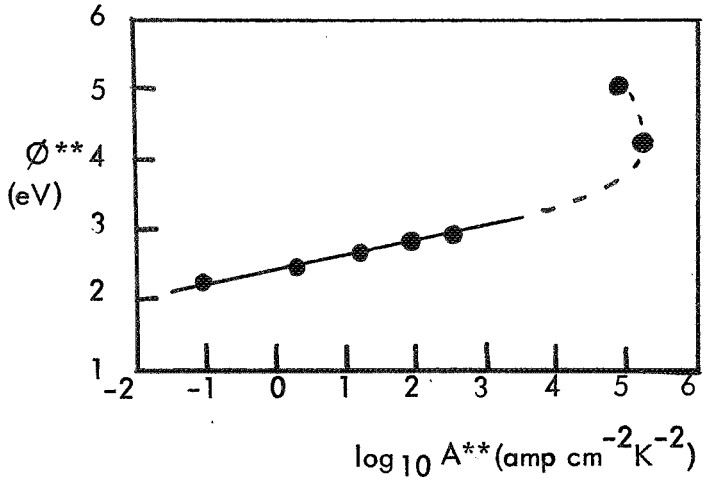

Figure 2.15. Compensation between Ø** and log A**

Figure 2.15 shows a plot of Ø** vs log A**. Full compensation between the two terms is obtained after the second point during carburisation. Hence, if we can conclude that a surface phase change (from W_2C to WC) has occurred beyond the maximum of the resistance curve, then the work functions for W_2C and WC must be very similar.

2.3.9. Contact potential difference (C.P.D.) measurements.

2.3.9.1. Chemisorption of Neopentane on Tungsten.

Figure 2.16 shows the change of C.P.D. with time when neopentane was leaked into the system containing a clean tungsten ribbon (Ø assumed to be 4.55 eV) and a gold reference electrode. The points marked A_1, A_2 and A_3 indicate admission of neopentane, B_1, B_2 and B_3 correspond to points when the system was pumped, and C_1 and C_2 indicate two minute heatings of the surface to 1640K and 1950K respectively; it is assumed that the

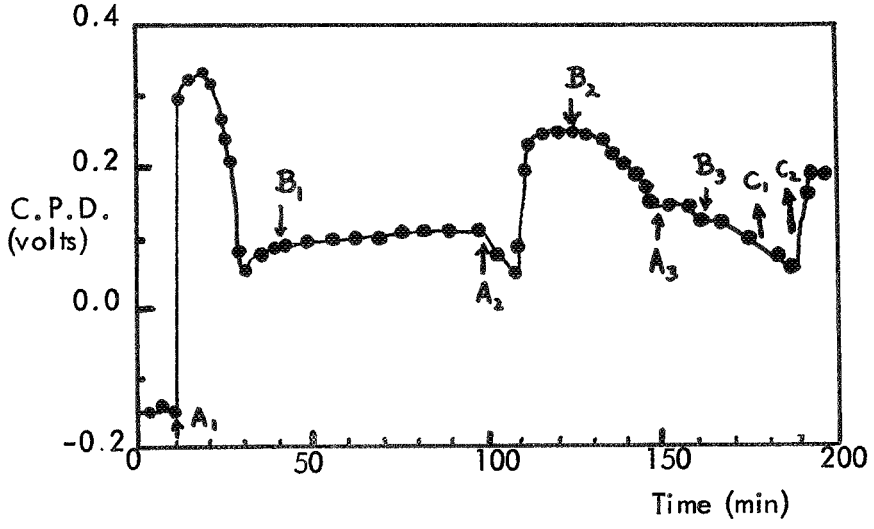

Figure 2.16. C.P.D. changes on chemisorption of $C(CH_3)_4$ on tungsten at 300K. A_1, A_2, A_3 - admission of $C(CH_3)_4$; B_1, B_2, B_3, system pumped; C_1 (C_2), tungsten heated to 1640K(1950K).

latter manipulation regenerated an essentially clean tungsten surface. Initially, there was a rapid rise of C.P.D., with a subsequent slow decay. When the system was subsequently pumped (B_1) there was a small rise in C.P.D. Further addition of neopentane (A_2) resulted in a fall of C.P.D. corresponding to the rise after pumping, and then there was a further rise, which fell when the system was pumped again (B_2). Further addition of neopentane and then pumping the system had little effect. Heating the ribbon likewise had little effect.

Neopentane is dissociatively chemisorbed by tungsten at room temperature by a rapid process.[7] After several minutes, the average surface composition has been shown, by hydrogen-deuterium exchange methods, to be about C_5H_8; it was not possible to ascertain the extent of C - C bond cleavage in this adsorbed species. In order for this species to be formed, the neopentane molecule must initially lose one hydrogen atom and form a single bond to the surface. Then other carbon-hydrogen bonds will be broken and multiple bonds will be formed on the surface. Such a process was not detected in the hydrogen-deuterium exchange experiments. However, the rapid rise in C.P.D. followed by a slower decay is probably indicative of this series of steps; C_5H_{11} radical initially formed will have a relatively high dipole moment, and as it breaks down, so the dipole moment decreases. When the system is pumped, there is a further small increase in the C.P.D.; this is probably due to the desorption of hydrogen noted in the earlier work. The addition of further neopentane (A_2) causes a further increase of the C.P.D.; this is equivalent to the first rapid increase and is due to largely undissociated radicals chemisorbing on the sites vacated by the hydrogen which was removed on pumping. When the system was pumped again, (B_3) the C.P.D. falls rather than the rise noted earlier; thus, this must be due to a combination of desorption of hydrogen and rearrangement of the larger dipoles on the vacated sites. Further addition of neopentane (E_3) and pumping (B_3) has little or no effect. Hence the surface is now covered by relatively stable species.

When a surface covered by adsorbed species was heated, both hydrogen and methane are desorbed[7]; the temperature was such that only carbon can remain on the surface,

and this will diffuse into the bulk, leaving a clean tungsten surface. The C.P.D. is now changed from the clean surface value by about 0.3 volts. The change must be attributed to a change in the work function of the gold electrode, probably due to a weak adsorption of neopentane. That this was the case was shown by baking the system, when the C.P.D. changed back to the original value. Hence all the C.P.D. changes discussed above are altered by this change of 0.3 volts on the reference electrode. However, this does not affect the arguments put forward; allowance for the change is made below when the change of work function during the carburisation process is discussed.

2.3.9.2. Formation of bulk carbides.

Figure 2.17 shows the change in C.P.D. observed with partially and completely carburised tungsten filaments. C.P.D. measurements could only be made with the ribbon cold; the cooling of the ribbon (in vacuo) is shown by the arrows at points 1, 2 and 3. The extent of carburisation was shown by resistivity measurements.

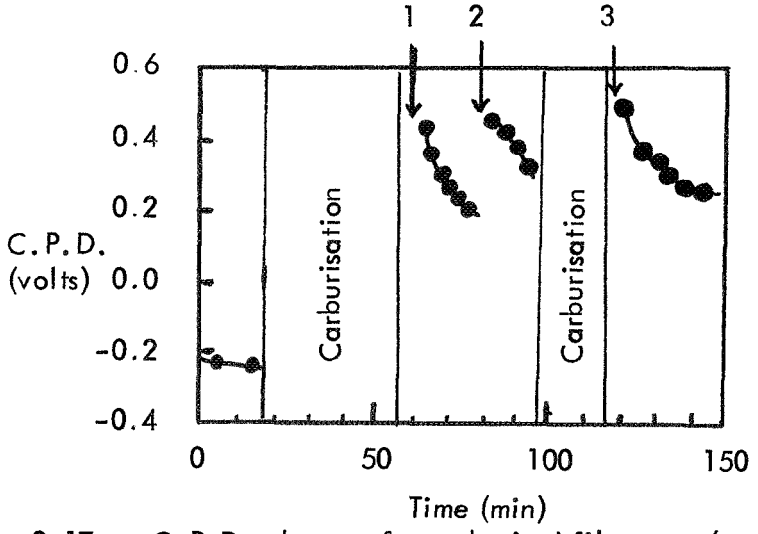

Figure 2.17. C.P.D. changes for carburised filament. (see text).

The ribbon was initially carburised to about 40% (W_2C) in neopentane at ~2000K. The system was then pumped and the ribbon was cooled. Subsequently the C.P.D. was ~+0.5 volts but fell slowly to ~+0.3 volts. When the ribbon was heated again and cooled (point 2), this time in a background pressure about half of that at point 1, ($\sim 10^{-7}$ torr) the C.P.D. fell more slowly to about 0.4 volts. Hence, the fall in

C.P.D. is thought to be associated with the adsorption of the background pressure of neopentane on the carburised ribbon. Hence a value of about +0.5 volts corresponds to the clean carburised ribbon. The value of the C.P.D. on complete carburisation is shown by the behaviour after point 3, which is similar to that after points 1 and 2. The value of the C.P.D. before adsorption of background neopentane is now about +0.55 volts.

Assuming that the value of the work function of the clean ribbon was initially 4.55 eV, the value of the work function of the gold electrode in the mercury pumped system (not the same as for clean gold) is about 4.80eV (i.e. C.P.D. $\simeq$ -0.25 volts). Allowing for the adsorption of the neopentane on gold discussed above (C.P.D.$\simeq$+0.3volts) and the change of C.P.D. on carburisation (+0.55 eV), the work function of the carbide is around 5.05eV. (i.e. 4.55 + 0.25 - 0.3 + 0.55 eV). This result was checked by making C.P.D. measurements in a system free from neopentane. A ribbon was reacted to completion in neopentane at 2000K, as indicated by resistance changes, and the system was then baked with the traps maintained at 195K. Assuming that the clean gold work function was 4.8eV, the steady measured value of C.P.D. obtained of +0.25 indicates an identical value of 5.05eV for the work function of the carbide formed.

2.4. CONCLUSIONS.

It has been shown that a tungsten filament becomes carburised during the interaction of hydrocarbon gases at higher temperatures. Initially W_2C is formed, but WC formation also occurs. The application of a field increased the rate of carburisation in the presence of neopentane, but has little or no effect with butadiene and tetramethylsilane. The apparent (thermionic) work function of both W_2C and WC is about 2.5 eV, but the average work function is about 5.05 eV.

REFERENCES

1. M. W. Roberts, J. R H. Ross, J. H. Wood and W. J. Murphy, Final Report to T.R.W. Systems, October 1969.

2. M. W. Roberts, J. R. H. Ross and J. H. Wood, Final Report to T.R.W. Systems, October 1968.

3. H. A. Jones and I. Langmuir, General Electric Review, 30, 310, (1927).

4. M. R. Andrews, J. Phys. Chem., 27, 270, (1923).

5. J H. Wood, Ph.D. Thesis, University of Bradford, 1970.

6. B. T. Barnes, J. Phys. Chem., 33, 688, (1929).

7. C. Kemball, M W. Roberts, and J. R. H. Ross, to be published. J. R. H. Ross, Ph.D. Thesis, Queen's University of Belfast, 1966.

3.0. THE USE OF RHENIUM AS A FILAMENT MATERIAL

3.1. INTRODUCTION

Earlier work (see Part 1) showed that when tungsten was used as an emitting filament for the electron beam polymerisation process, carburisation of the filament occurred, and this reaction gives rise to a change in the work function of the filaments; a more detailed investigation of the process is reported in Part 2. In order to study the kinetics of the polymerisation process, it is desirable to have a filament with a constant work function. It has been claimed that rhenium does not form a carbide, and that only a solid solution of carbon in rhenium is formed.[1] A carbide of rhenium has been reported by several authors,[2] but the evidence for these claims has been dismissed.[3]

It was therefore proposed to use rhenium as a filament material for a study of the kinetics of negative ion formation, initially using a magnetron cell[4] to examine the variation of negative ion current as a function of the reaction conditions. However, it was found that the resistance of the rhenium filament changed quite considerably when the filament was heated in a hydrocarbon atmosphere (neopentane) and it was also found that the work function of the filament changed during reaction.

Part 3 therefore reports a detailed investigation of the reaction of rhenium at high temperatures in a low pressure of neopentane, in an attempt to determine whether a carbide of rhenium is formed. The evidence to be presented indicates that at least one carbide of rhenium is probably formed, and once the carburisation reaction has proceeded to a certain stage, the emission characteristics of the filament become constant, allowing such a filament to be used for a kinetic investigation. The following types of measurement have been made in order to identify the change in filament composition :-

(a) hot and cold resistance changes,

(b) emission changes in the presence of neopentane,

(c) vacuum emission at various stages of reaction,

and (d) measurement of temperature variation of resistivity at various stages of reaction.

In addition, X-ray powder photographs were taken of filaments reacted to various extents, and photomicrographs of the surface structure of the filaments at the same extents of reaction.

3.2. EXPERIMENTAL.

The system used was the magnetron apparatus described in an earlier report. The magnetron cell itself was modified. Instead of the anode made of nickel foil, a tungsten film evaporated on the inside of a cylindrical glass tube was used, and the grid structure was simplified. The filament 0.25 mm diameter pure rhenium wire supplied by Koch-Lite Ltd., was suspended under tension between two tungsten supports. The magnetron cell was part of a bakeable flow system pumped continuously by an oil diffusion pump. The oil was excluded from the magnetron cell by a trap maintained at 193K. Neopentane, of research gradesupplied by Matheson Co. Inc., was leaked continuously through a capillary leak to give a continuous pressure of the order of 10^{-3} torr. Reaction was examined with the filament at temperatures initially between 1850 and 2200K, and using constant A.C. heating currents. The temperatures quoted for each experiment therefore correspond to clean rhenium temperatures (determined with an optical pyrometer), and the temperature during any one experiment rises slightly with time due to the increase of filament resistance (see below).

Cold resistance measurements at various stages of reaction were made by cooling the filament and using a Wheatstone bridge circuit. Hot resistance changes were monitored by means of a rectifying circuit which allowed the potential difference across the filament to be recorded continuously. Vacuum emission characteristics were obtained at various stages of reaction, after interrupting the supply of neopentane. The variation of resistivity with temperature during these measurements was obtained using the rectifying circuit described above. Emission either during reaction or in vacuum was recorded on

a second recorder, and these two recorders enabled the time dependent decay processes observed in some cases to be followed.

X-ray measurements were made using a Debye-Shewer powder camera, using nickel filtered copper (K_α) radiation. Surface photographs were taken using a Vickers projection microscope giving a total magnification of approximately 2000 times. Both sets of data were obtained with filaments reacted for a definite time and then removed from the magnetron cell. Some experiments were carried out on filaments which had already been reacted and were subsequently outgassed at high temperatures (~2500K, with flashing to higher temperatures) before the experiment; resistance measurements, coupled with vacuum emission measurements, showed that such a filament was essentially pure rhenium.

3.3. RESULTS AND DISCUSSION .

3.3.1. Resistance Changes.

With reaction at a constant heating current, the cold resistance at various stages of reaction was found to increase rapidly to a peak value, followed by a slight drop. Similar behaviour was obtained with and without an applied field during reaction. Figure 3.1. shows schematically some typical data. The hot resistance data were found to be similar (figure 3.2).

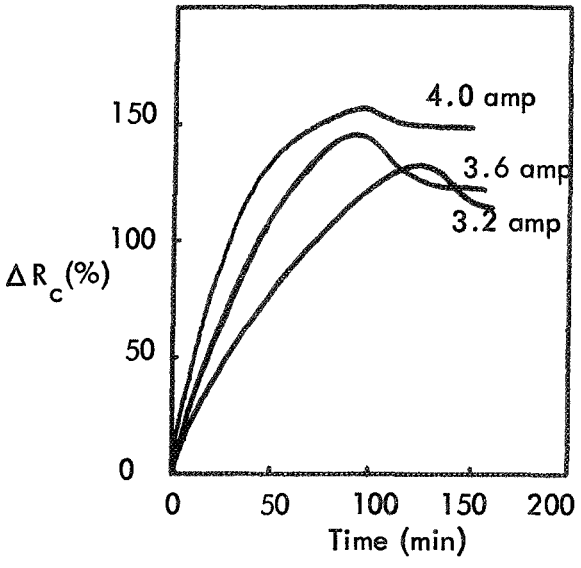

Fig.3.1. Cold resistance changes for carburisation at different temperatures.

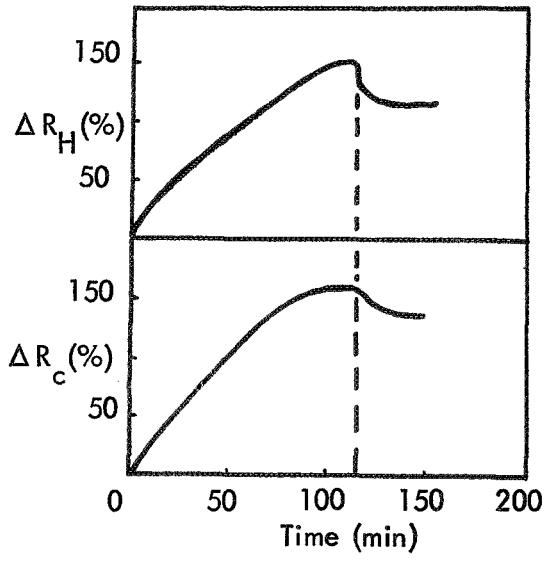

Fig.3.2. Comparison of hot and cold resistance changes for carburisation at 3.2 amp.

A continuous increase of filament resistance of the type shown in figures 3.1 and 3.2 is compatible with the introduction of an alloying agent which results in centres of lattice distortion and consequent scattering of electrons by these centres. Hence, the initial resistance increase is taken to indicate the steady diffusion of carbon from the surface into the bulk phase. As the monomer contains only carbon and hydrogen, only carbon contamination is likely. The drop in resistance observed after the maximum must indicate some reordering of the bulk structure and must be interpreted as a bulk phase change (see section 3.3.2), as it is unlikely that a resistance drop of the magnitude observed could be caused by a surface change such as deposition of graphite.

3.3.2. Total Emission Measurements during Reaction.

Although in principal the magnetron could be used to distinguish the electron and negative ion currents during reaction, only total emission current measurements have been made. Figure 3.3a shows typical data obtained and figure 3.3b shows the corresponding cold resistance data. The emission current behaviour shows three distinct stages. In Stage 1, the emission current drops slightly and then remains constant

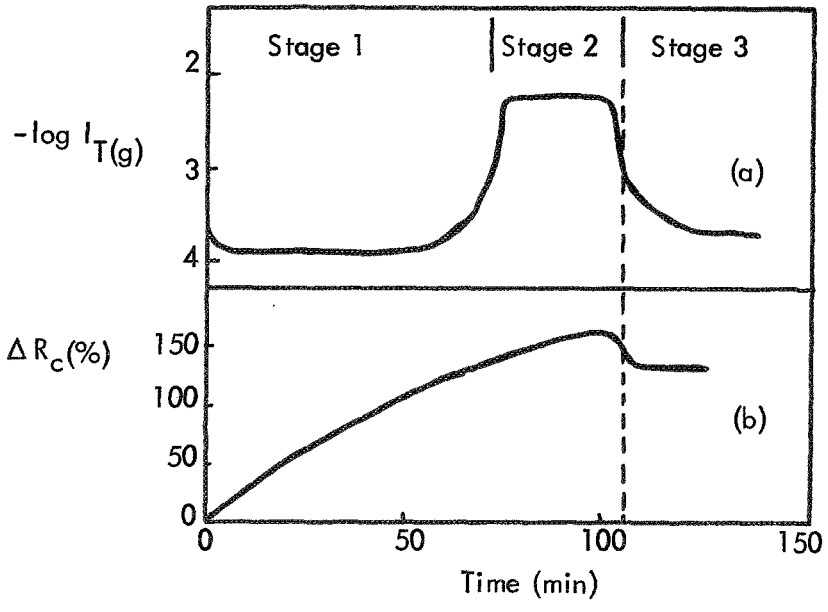

Figure 3.3. Comparison between emission and cold resistance changes for carburisation at 4.0 amp.

for a period of about sixty minutes. A sharp rise in emission then occurs and the current levels out at a value about 300 times the value in stage 1; this is designated as stage 2. The time for which stage 2 lasted was between 20 and 100 minutes, and depended on the filament temperature, i.e. most probably on the rate of diffusion of carbon into the filament. The emission then decays to a level comparable with that observed in stage 1 (stage 3). The drop in emission from stage 2 to stage 3 was found to correspond to the drop in cold resistance (compare figure 3.3b); no definite change in resistance was found which corresponded with the change from stage 1 to stage 2, but it is probable that there is a change in the temperature coefficient of resistivity at this point, indicating a phase change at this point also. Hence, it is inferred that the changes in total emission are indicative of bulk phase changes rather than changes in the surface composition alone.

Figure 3.4 shows more detailed data for the total emission at various filament temperatures.

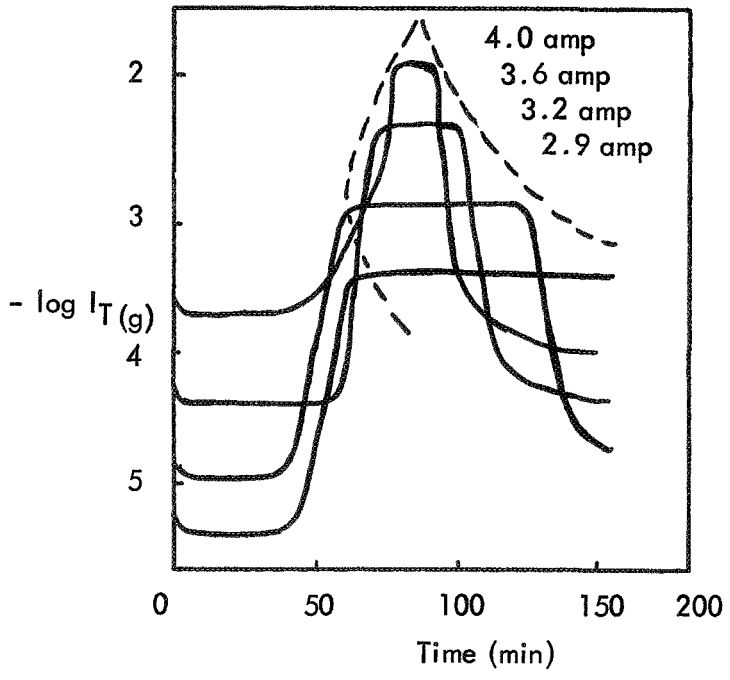

Figure 3.4. Emission changes in the presence of gas for carburisation at different temperatures.

The time for which the stage 2 emission is observed decreases with increasing filament temperature. These results are completely reproducible. If it is assumed that the

rate of diffusion of carbon into the bulk remains approximately constant from stage 1 through to stage 3, and that this rate increases with increasing filament temperature, then as the time for which the phase corresponding to stage 1 persists is approximately constant, it must exist over larger composition ranges with increasing temperature. This phase could correspond to the α -rhenium solid solution characterised at higher temperatures by Hughes.[1] Apart from the X-ray data and the data on the surface appearance given below, no evidence has as yet been obtained for the nature of the phases present during stages 2 and 3. Further work designed to characterise the phases is proceeding at present.

3.3.2. Vacuum Emission Measurements.

In order to determine the work function of the filament during carburisation (ϕ^{**}, see Part 2), vacuum emission characteristics ($\log I_{T(v)}$ vs $1/T$) were obtained at intervals during reaction. Unusual behaviour was obtained, as shown in figures 3.5 and 3.6, but this was completely reproducible. Figure 3.5 was obtained when the filament was carburised at a temperature of 1960K and figure 3.6 was obtained by carburisation at 2170K. At t = 0 and early in stage 1, straight lines are obtained, but later in stage 1, the emission deviated from the straight line of the Richardson equation,

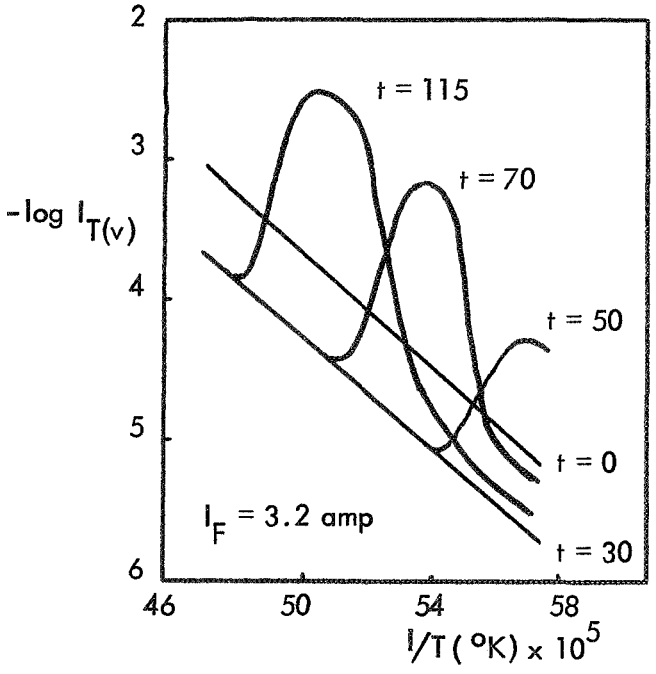

Figure 3.5. Vacuum emission characteristics of partially carburised filaments.

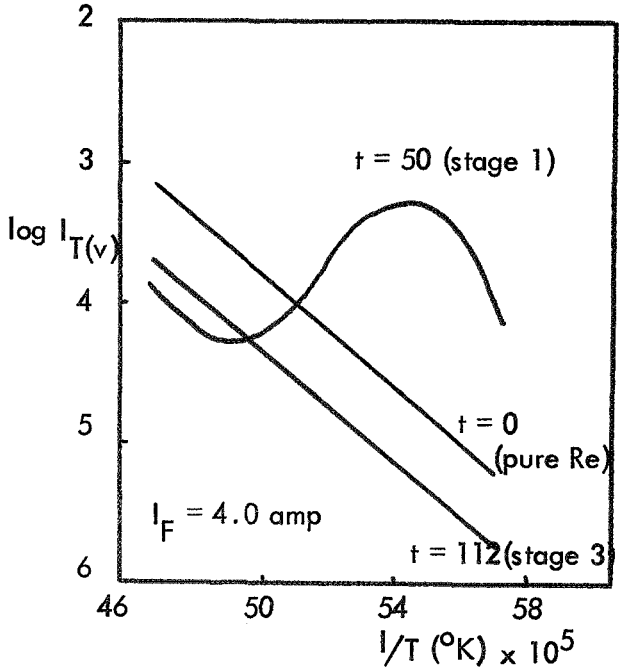

Figure 3.6. Vacuum emission characteristics at the various stages of reaction.

There is a temperature region in which an apparent "negative work function" region exists; in this region, the emission increases when the filament temperature is lowered. A "stage 3 filament" (i.e. a filament reacted to stage 3 emission) again gave a straight line Richardson plot, but a "stage 2 filament" may give either type of behaviour.

In the apparent negative work function region of temperature described above, when the filament temperature was lowered, there was the expected rapid drop in emission which occurred with a normal filament, but then the emission increased slowly over a period of several minutes to a value greater than that at the higher temperature. It is such steady emission currents which are plotted in figures 3.5 and 3.6. In the lower temperature regions, a different tupe of behaviour was observed: when the temperature was lowered, there was the normal rapid fall followed by a slower decay process. Figure 3.7 shows a typical Richardson plot for data obtained at this stage of carburisation, and also shows, by means of the arrows drawn for each incremental temperature decrease, the behaviour of the emission current where the temperature was decreased.

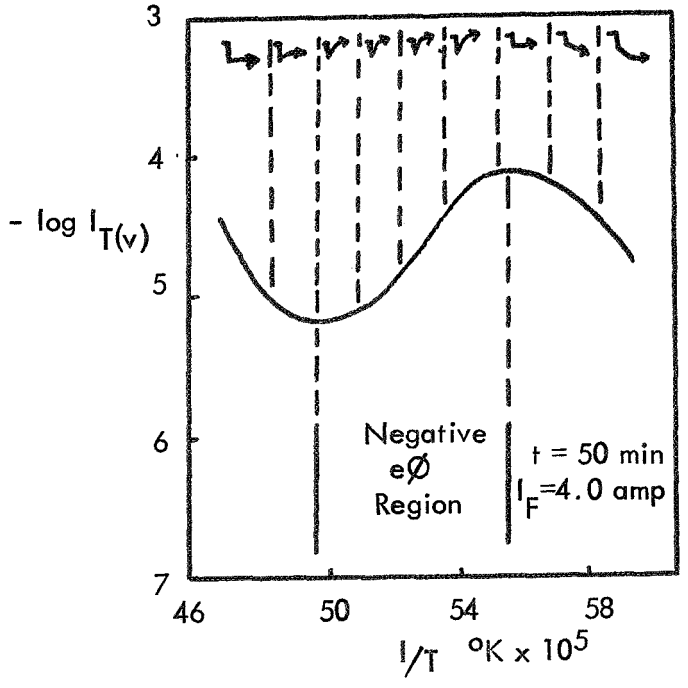

Figure 3.7. Decay curve behaviour in the different regions of vacuum emission from a stage 1 filament.

The unusual emission characteristics and the alteration of the emission current with time must be explained in terms of the impurity content of the filament. In the early stages of stage 1 behaviour, the filament composition will probably correspond to an α-rhenium solid solution at all temperatures at which emission was measured. However, later in stage 1, when the filament is cooled, the limiting solubility will be reached at a certain temperature. (The solubility increases with increasing temperature.[1]) From that temperature downwards, carbon will continue to either precipitate out as graphite or form a new carbide phase; as the effect is for the emission to increase, the latter is more probable. If the emission from the carbide is lower than from α-rhenium at lower temperatures, then the slow decay in this region is also explained. Once stage 2 is reached, the carbide already exists. Early in this stage, changes in temperature will cause relatively large changes in the proportion of carbide, but later on, the carbide concentrations are so high that the α-rhenium concentration change on cooling is negligible. This means that the filament comprises essentially a single material, and so approximately straight line Richardson plots are again obtained (t = 112 mins, figure 3.6). In stage 3, yet another carbide structure may exist (see above), and so the straight line Richardson plots must again infer that no change in the phase compositions occur in this region. The apparent work function (ϕ^{**}) calculated for a stage 3 filament was 5.5 eV.

3.3.3. Temperature Coefficient of Resistivity.

In an attempt to show if any bulk phase changes occurred during the emission changes (essentially a surface property), the hot resistances of the filaments were measured as a function of temperature at various stages of carburisation. Figure 3.8 shows typical data obtained during the latter part of stage 1 behaviour. The emission current and the "decay behaviour" are also shown. A definite discontinuity in the resistance/temperature plot occurs at the stage when the emission starts to decay on decreasing the temperature. With pure rhenium or a carburised filament which gave straight line Richardson plots, straight line resistance/temperature plots were obtained. This result is therefore further evidence for the presence of a carbide of rhenium other than a solid solution.

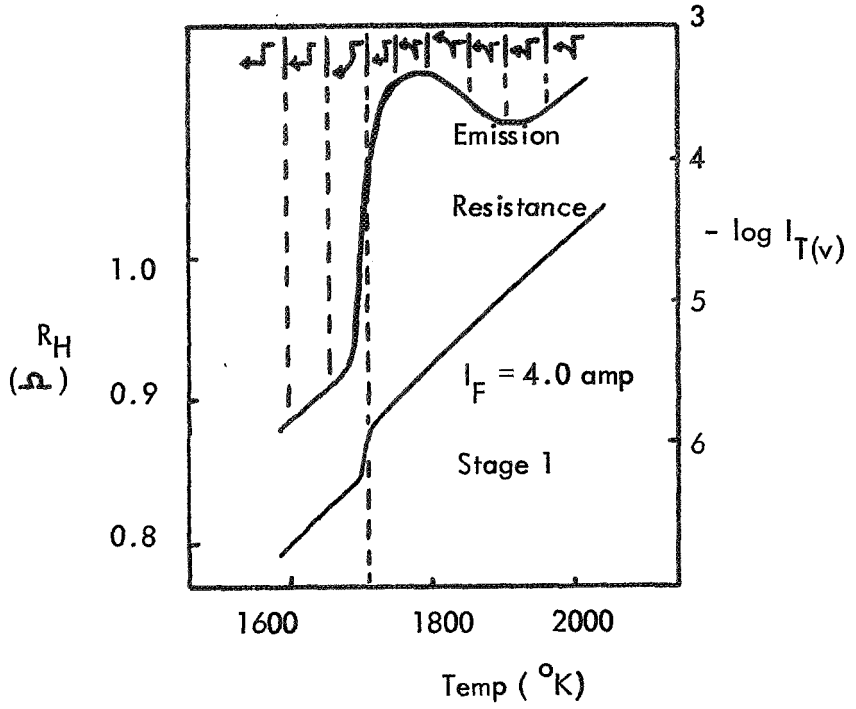

Figure 3.8. Comparison of hot resistance, vacuum emission and decay curve changes with temperature for a stage 1 filament.

3.3.4. X-ray Spectra .

X-ray photographs were taken at various stages of reaction in a further search for evidence for the existence of a carbide or carbides of rhenium (see figure 3.9). The filament retains a close packed hexagonal structure throughout the reaction, but variations in the line positions are evident, more particularly at high angle reflections, where two separate rings appear and continue to grow during the reaction. If the

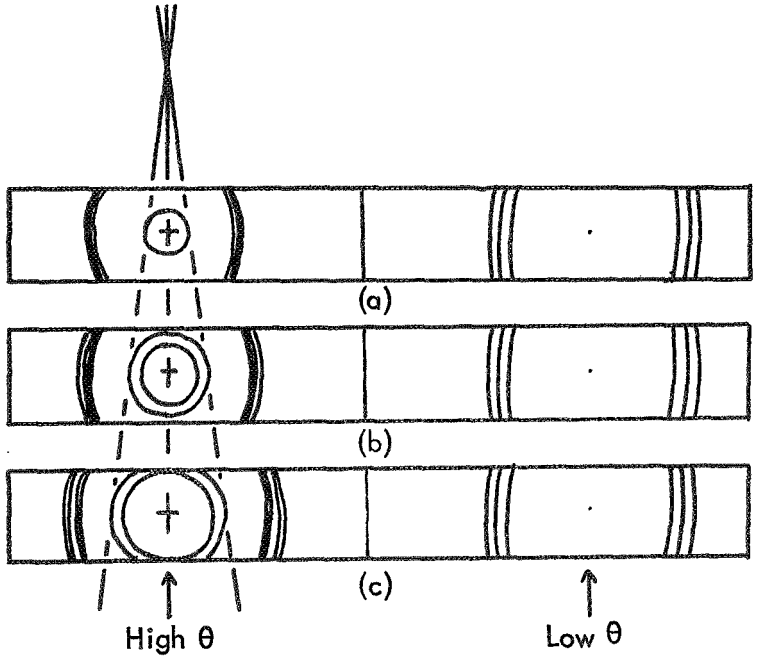

Figure 3.9. Schematic comparison of changes observed in some of the more intense X-ray lines on carburisation.
(a) Pure outgassed Re
(b) Stage 1 filament
(c) Stage 2 filament

rhenium structure did not have to change to accommodate carbon as a carbide, and the migration of carbon into the bulk occurred with a slight expansion of the lattice, then these results are further evidence for carbide formation. However, lattice expansion is probable even with the formation of α-rhenium.

3.3.5. Changes of Surface Appearance.

Plates 3.1 to 3.4 show surface microphotographs, at magnification about 2000X, taken at various stages of reaction. Plate 1 shows the surface of a new, well-outgassed rhenium filament. The circular dots on the surface would appear to be due to contamination, and could be found on most of the filaments examined. The lines running from left to right appear to be shallow depressions on the surface and are probably surface scratches caused during the drawing process. An irregular pattern also appears on the surface, and these are probably grain boundaries. Plate 2 shows the surface of a filament during stage 1 of reaction. The lines due to drawing still exist and a more regular pattern of grain boundaries exists. Plate 3 shows the surface of a filament at stage 2 and plate 4 shows the surface of a filament reacted to stage 3. In both of these photographs, smaller grain boundaries have appeared within the larger grains and the drawing marks have disappeared. The smaller grains could be indicative of a new phase, but they could also be caused by a thermal etching process. There is no evidence of graphite on the surface. It is hoped that more conclusive evidence for a new phase might result from examination of cross-sections of the filaments.

3.4. CONCLUSIONS.

Contrary to expectation, rhenium appears to form a carbide with a work function different from that of clean rhenium. However, the emission behaviour of such a filament is very different to that of tungsten and its carbides (see Part 2.) Partially carburised tungsten always gave emission obeying the Richardson equation ($\log I \propto T^{-2}$) and changing continuously during carburisation. In contrast, rhenium gave emission which indicated the existence of phase changes during temperature cycling. Hence, it would appear that diffusion of carbon throughout the whole filament is relatively rapid, and phase equilibria are established readily throughout the bulk. Once the

extent of carburisation is high, the filament again obeys the Richardson equation i.e. it behaves as a pure material. At this stage, the filament is a stable emitter and is suitable for use in a study of the kinetics of the formation of thin polymer films. It would seem desirable to confirm the existence of a carbide (or carbides), and this should be possible using chemical methods.[5]

REFERENCES.

1. J. E. Hughes, J. Less Common Metals, 1, 377, (1959)

2. A. J. Evstyukhin et al., Met. i Metallovia. ChistykhMetal., St. Nauchm. Rabot, 1963, (4) p.149.

3. D. J. Maykoth et al., Tech. Rpt. AFCRC-TR-60-153 (PB149169), 1960.

4. M. W. Roberts, J. R. H. Ross, J. H. Wood and W J. Murphy, Final Report to T.R.W. Systems, 1969.

5. I. J. McColm and J. S. Anderson, (Private communication).

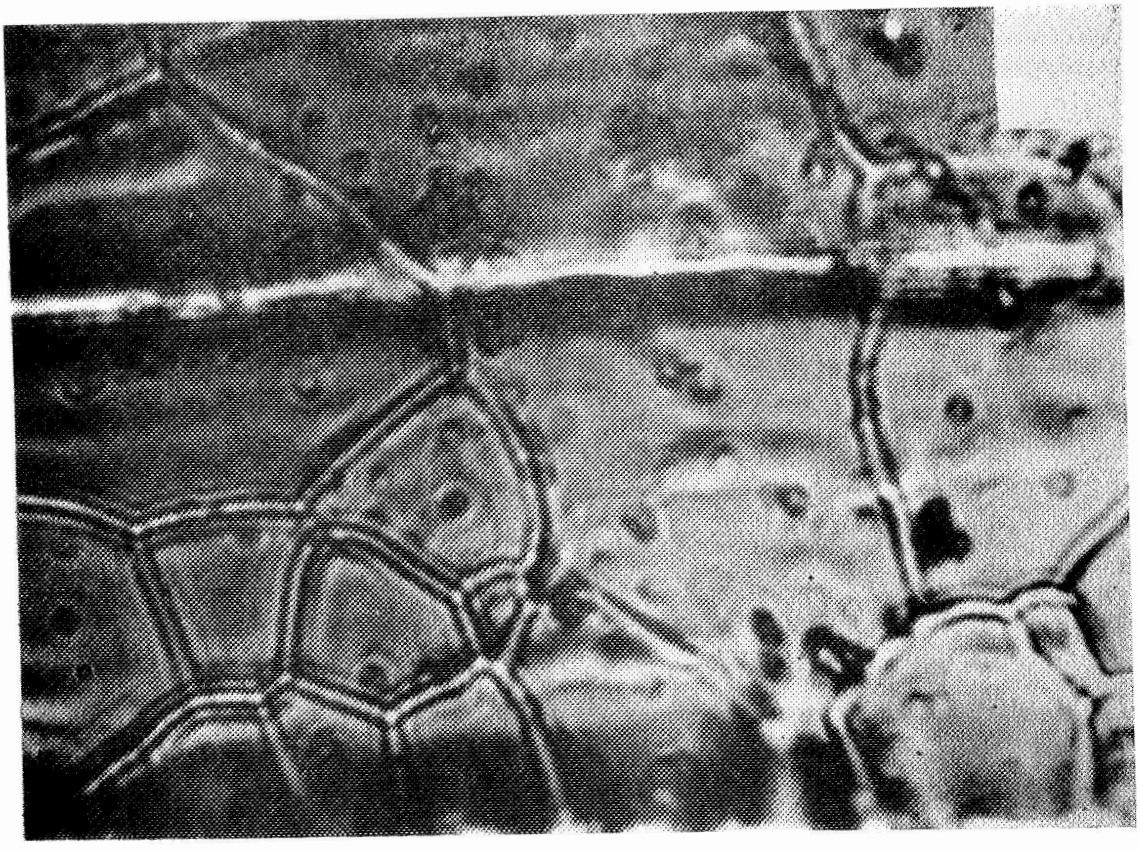

PLATE 1

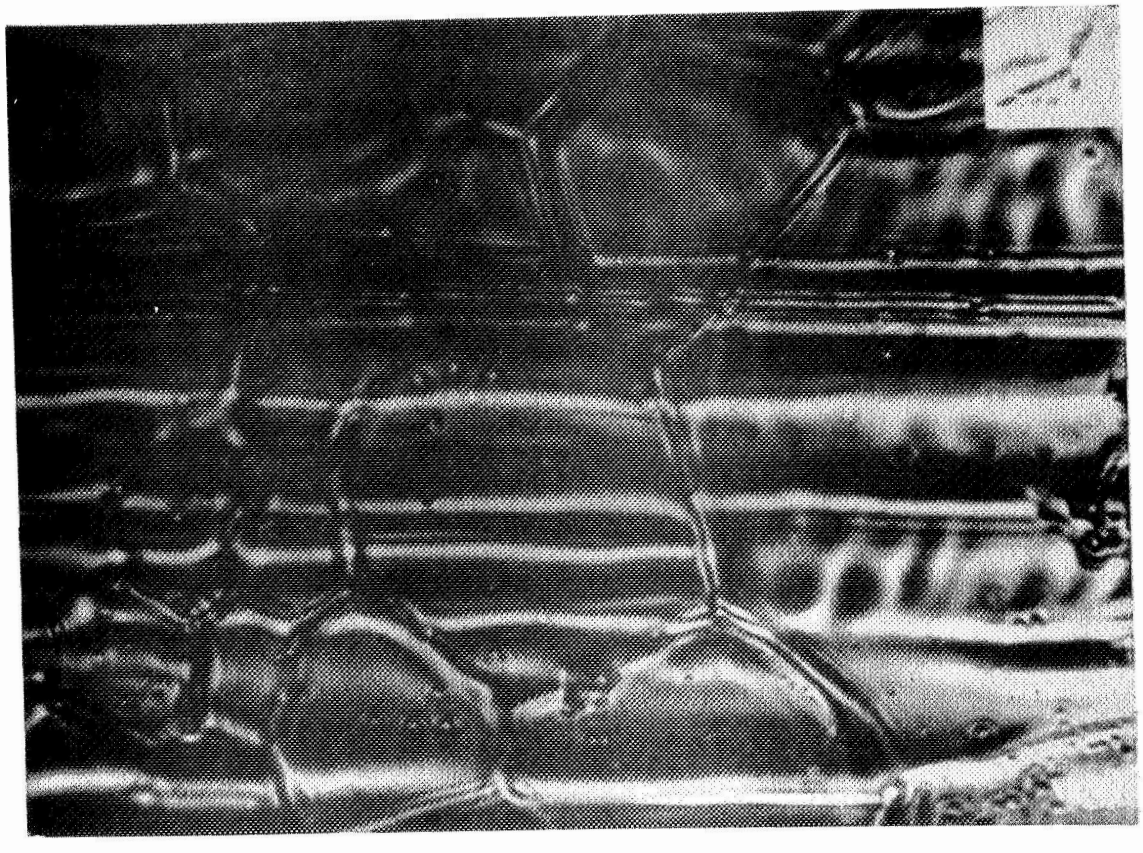

PLATE 2

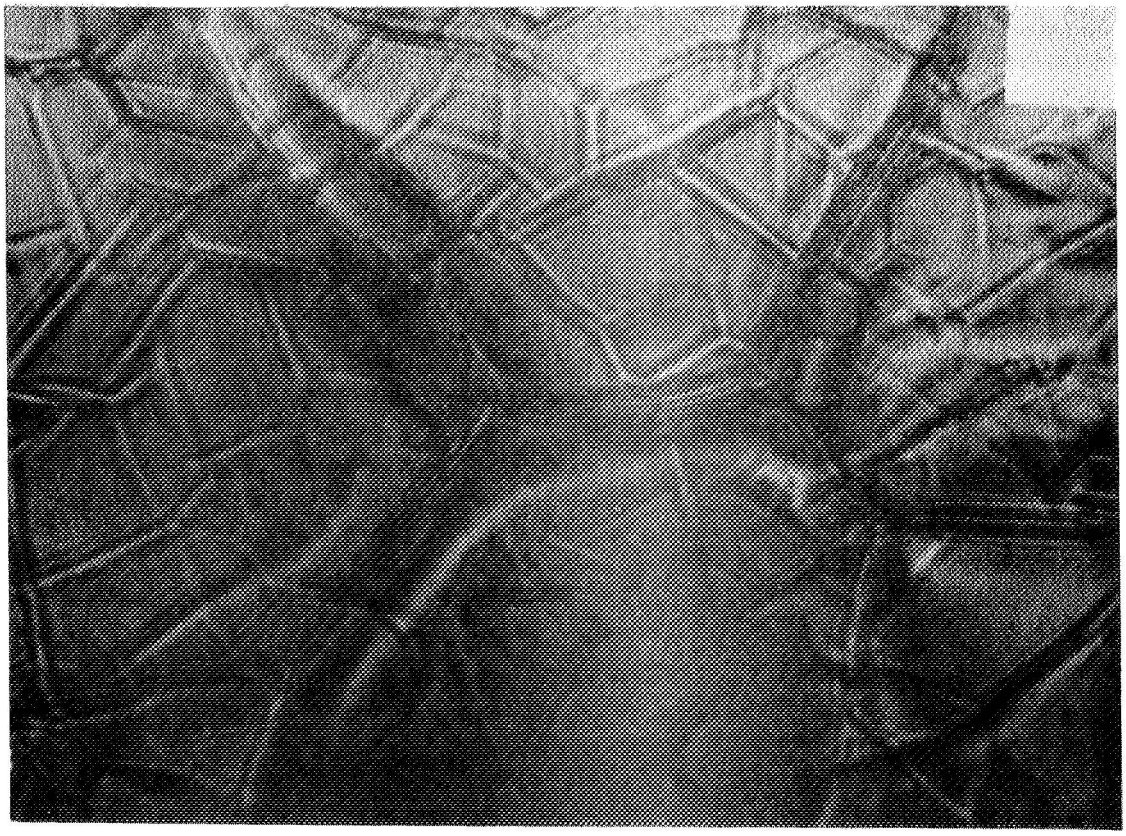

PLATE 3

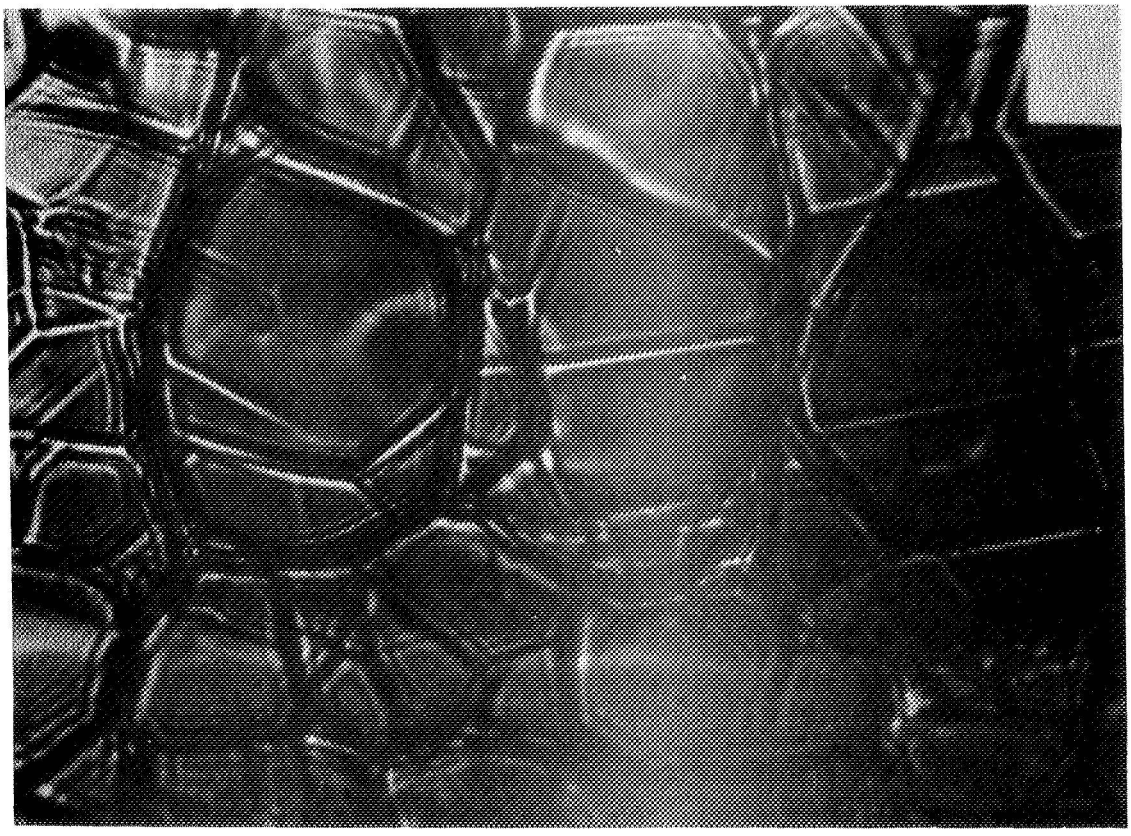

PLATE 4

4.0. STUDY OF THE SURFACES OF POLYMERIC MATERIALS.

4.1. INTRODUCTION .

It was shown in the last annual report[1] that contact angle measurements could be used to help to characterise the surface of the thin polymeric films prepared by the electron bombardment process (see section 1.2.8). It was also shown that when dilute aqueous solutions of aliphatic alcohols were used instead of pure liquids, different results were obtained. These were explained by postulating that adsorption of alcohol molecules occurred on the surface of the polymers, and the surface was subsequently characteristic of the outermost groups of the adsorbed molecules.

A theory was presented to enable the contact angle measurements to be treated quantitatively. This was based on work by Fowkes and Harkins[2] which made the basic assumption that adsorption occurred only at the solid-liquid interface formed by the drop and that no adsorption occurred at the liquid-vapour interface. This assumption has been shown to be untenable, and so in this report (section 4.2 below) we present a modified form of the theory, which takes adsorption from the vapour phase into account. Subsequently (section 4.3) we present data which show that this theory applies to two model systems, polystyrene and polymethylmethacrylate. This involves a separate study of the adsorption of butanol from aqueous solution on the surface of powders of the two polymers; the results obtained are completely in agreement with predictions made from contact angle measurements carried out on flat surfaces of the two polymers[3].

Contact angle measurements have been carried out on a large variety of thin polymeric films prepared from perfluorobutene-2 using various different preparation conditions. These results are presented in section 4.4 below. Section 4.5 presents some data relating polymer film thickness to preparation conditions.

4.2. THEORY AND METHOD OF THE INTERPRETATION OF RESULTS FOR CONTACT ANGLE MEASUREMENTS USING DILUTE AQUEOUS SOLUTIONS.

For a drop of liquid on a solid surface (see figure 1.1), the Young-Dupre equation (see ref.4) is

$$\gamma_{SV} = \gamma_{SL} + \gamma_{LV} \cos\theta \qquad \ldots\ldots(4.1)$$

Differentiating with respect to ln a, where a is the activity of the solute in the solution, we obtain

$$\frac{d(\gamma_{LV} \cos\theta)}{d \ln a} = \frac{d(\gamma_{SV} - \gamma_{SL})}{d \ln a} \qquad \ldots\ldots(4.2)$$

The Gibbs Adsorption isotherm for any interface (equations 4.3 and 4.4) relates the change in surface tension at that interface with the change in a to the value of the

$$\frac{d\gamma_{SL}}{d \ln a} = -RT(\Gamma_2)_{SL} \qquad \ldots\ldots(4.3)$$

$$\frac{d\gamma_{SV}}{d \ln a} = -RT(\Gamma_2)_{SV} \qquad \ldots\ldots(4.4)$$

surface excess of the solute, Γ_2, at the interface. Equation(4.3) applies to the solid-liquid interface whereas equation(4.4)applies to the solid-vapour interface. R is the gas constant and T is the absolute temperature. If equilibrium exists, the activity of the solute is the same in both liquid and vapour. At low activities, $\Gamma_2 \simeq n_2$, where n_2 is the concentration of solute molecules at the interface in question.

Substituting equations (4.3) and (4.4) in equation (4.2), we obtain

$$\frac{d(\gamma_{LV} \cos\theta)}{d \ln a} = RT \left\{ (\Gamma_2)_{SL} - (\Gamma_2)_{SV} \right\} \qquad \ldots\ldots(4.5)$$

As mentioned above, we have previously[1] assumed that $(\Gamma_2)_{SV} = 0$, but this is not necessarily the case. Hence we obtain in equation (4.5) a composite term, $\left\{ (\Gamma_2)_{SL} - (\Gamma_2)_{SV} \right\}$ when we examine the variation of $\gamma_{LV} \cos\theta$ with log a;

these data are readily obtained from the cos θ vs γ_{LV} data obtained with solutions of varying activity a.

Hence, the isotherms presented in the last final report[1] (which will be presented again below) relating a quantity N_a to the mole fraction of alcohol represent a composite isotherm, being the difference between the isotherms at the solid-liquid and solid-vapour interfaces. Only if one of these interfaces is present without the other is it possible to determine the individual isotherm; having determined one of the two, the contact angle data enables the other to be calculated. In section 4.3, we therefore present data obtained from the adsorption of butanol from aqueous solution on polystyrene and polymethylmethacrylate surfaces (solid-liquid interface only). The two polymers were first ground until high area powders resulted and these were then immersed in a series of butanol solutions and the extent of adsorption was measured. Gas-liquid chromatography was used to analyse the dilute butanol solutions before and after adsorption.* The areas of the powders were obtained using krypton adsorption at 78K, and hence the butanol adsorption data were converted into units of molecules adsorbed/100$\mathring{A}^2$ to enable them to be compared with the results from contact angle measurements. The adsorption data obtained are of a form predicted from an analysis of the contact angle data[3]. Hence, a similar analysis may be made of the data for thin films of polyperfluorobutene-2, where it is not possible to study either interface separately (see section 4.4).

4.3. RESULTS AND DISCUSSION .

4.3.1. Results for Polystyrene and Polymethylmethacrylate.

4.3.1.1. Polystyrene.

Figure 4.1 shows the plot of cos θ vs γ_{LV} obtained previously[1] for dilute butanol solutions on a bulk polystyrene sample. Figure 4.2 shows the corresponding plot of $\{(\Gamma_2)_{SL} - (\Gamma_2)_{SV}\}$ vs butanol activity, a.

* We would like to express our thanks to Dr. J. M. C Turner of this Department, for his help in making these measurements.

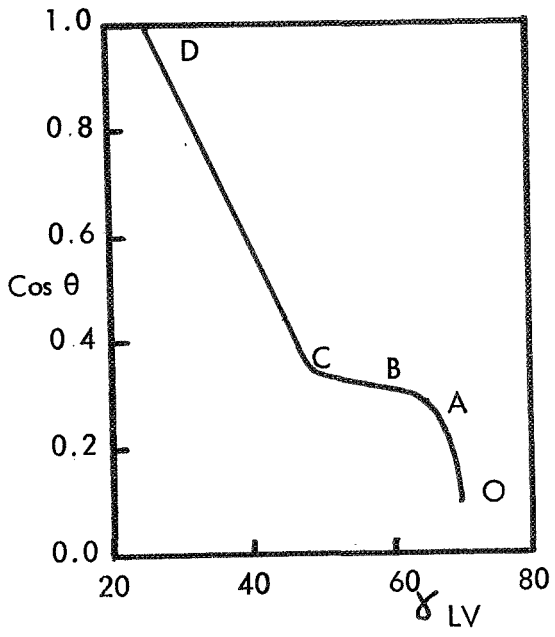

Figure 4.1. Contact angle data for dilute butanol solutions on polystyrene.

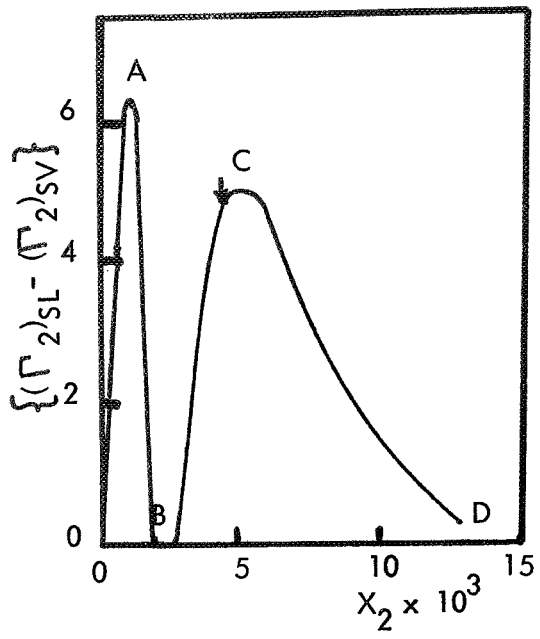

Figure 4.2. Plot of $\{(\Gamma_2)_{SL}-(\Gamma_2)_{SV}\}$ vs. X_2 for butanol solutions on polystyrene. (Γ_2)surface excess of butanol at the solid-liquid or solid-vapour interface; X_2 = mole fraction of butanol.

Figure 4.3 shows the krypton adsorption isotherm obtained at 78K on a powdered polystyrene sample. V is the volume of krypton adsorbed, P is the pressure of krypton with the sample and P_o is the saturation vapour pressure of krypton at 78K (2 torr). The area calculated for this sample, using the BET method and assuming that one krypton atom occupies an area of about 19.5$\AA^2$, is 1.5 $m^2 g^{-1}$.

Figure 4.4. shows the adsorption isotherm obtained for polystyrene immersed in butanol solutions, i.e. the solid-liquid interface only. The data take into account the area obtained in figure 4.3 and are expressed in (molecules adsorbed)/100$\AA^2$, which is compatible with the results in figure 4.2. Two steps are obtained in the isotherm, the first corresponding approximately to monolayer formation, and the second to the formation of several layers of butanol on the surface. The point X corresponds to the start of the

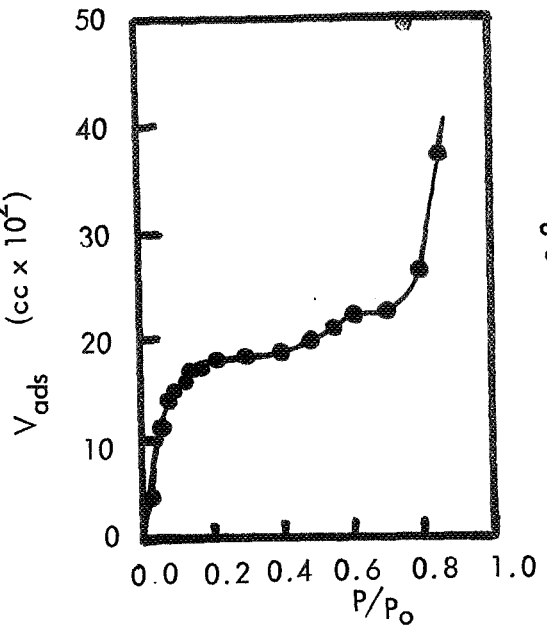

Figure 4.3. Krypton adsorption isotherm at 78K on powdered polystyrene

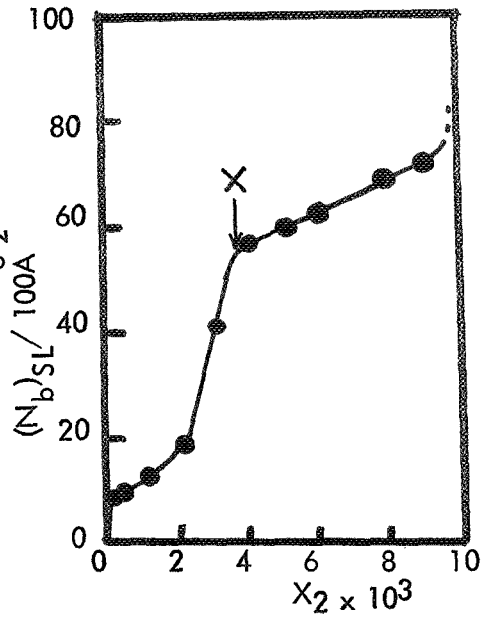

Figure 4.4. Plot of $(N_b)_{SL}/100\text{Å}^2$ $(N_b)_{SL}$ = no. of adsorbed molecules at solid-liquid interface vs. X_2 (mole-fraction of butanol in solution) for powdered polystyrene.

straight line section (point C) of the cos θ vs $_{LV}$ plot of figure 4.1. At even higher concentrations ($X_2 \simeq 0.012$), the coverage by butanol increases even further and this is approximately the point at which cos θ = 1, i.e. when the liquid spreads on the polymer surface. We would infer that at this point the character of the surface is unaffected by the nature of the underlying polymer, being entirely characteristic of the adsorbed multilayers.

The shape of the adsorption isotherm and magnitude of the adsorption at the two points of inflexion in figure 4.4 are entirely compatible with the results given in figure 4.2. Indeed, a two step isotherm similar to that in figure 4.4 was predicted in a quarterly report[3]. This prediction was made assuming that at low butanol concentrations, adsorption occurs first at the solid-solution interface, and when the adsorption is virtually complete at this interface, adsorption occurs at the solid-vapour interface; the adsorption at the solid-liquid interface must amount to at least 6 molecules 100Å^2

(point A, figure 4.2), and this is borne out by the results shown in figure 4.4. Once point B is reached (figure 4.2) further adsorption occurs at both interfaces in turn. The results of figure 4.4 show that this is multilayer adsorption, and this could not have been predicted solely from the results of figure 4.2. Figure 4.5 shows the isotherm calculated from the data of figures 4.2 and 4.4 for adsorption at the solid-vapour interface.

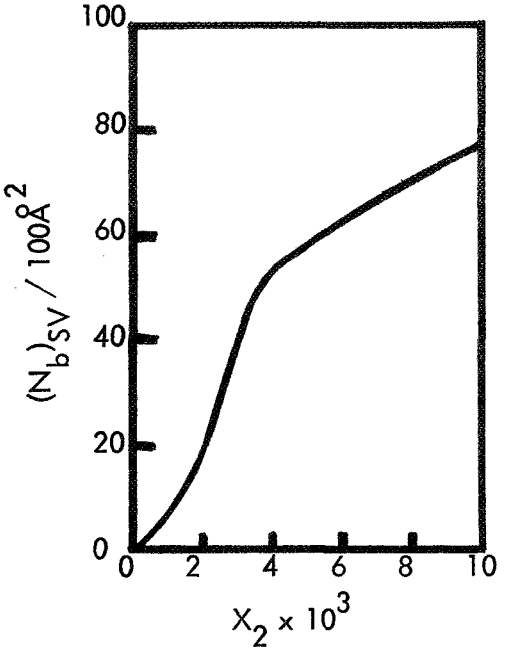

Figure 4.5. Calculated butanol adsorption isotherm for the solid-vapour interface.

The shape of the isotherm is very similar to that of isotherms obtained by Whalen[5] for the adsorption of hexane and octane on polytetrafluoroethylene at the solid-vapour interface. The first step in each isotherm indicates that a specific adsorption is occurring on the polymer surface, and this is likely to be dependent on the nature of the polymer. It will be seen below that no such specific adsorption occurs on the surface of polymethylmethacrylate. It is interesting to note that Bernett and Zisman[6] claimed that no adsorption occurred on low energy polymeric surfaces. Their conclusion has been used in at least one instance[7] in the interpretation of results of contact angle measurements on the surface of low energy solids. It is interesting to note that Bernett and Zisman[8] did invoke adsorption from solution in one system, namely fluorinated acids and salts on

polyethylene, but this conclusion has been ignored in subsequent publications (e.g.ref.3).

4.3.1.2. Polymethylmethacrylate.

Figures 4.6 to 4.10 show corresponding plots for polymethylmethacrylate. In figure 4.7, there is no initial peak corresponding to A in figure 3.2. It may therefore be inferred that we do not expect anything other than multilayer adsorption in this system.

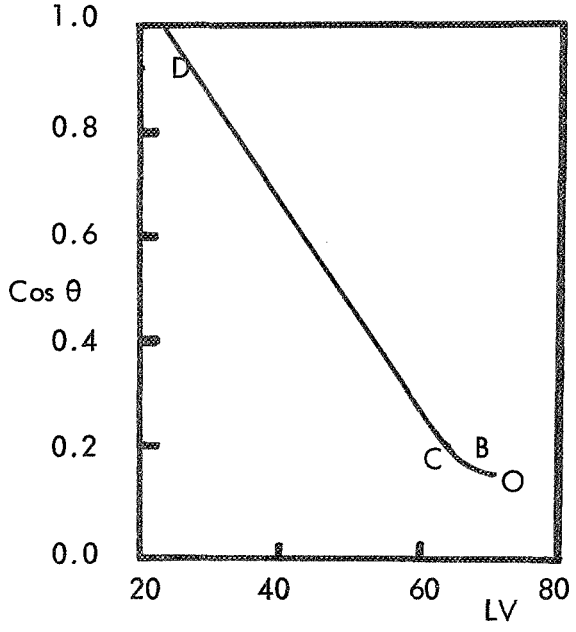

Figure 4.6. Contact angle data for dilute butanol solutions on polymethylmethacrylate.

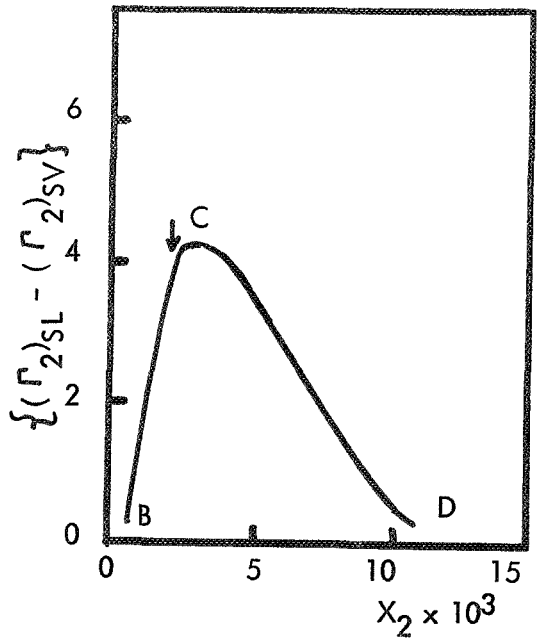

Figure 4.7. $(\Gamma_2)_{SL} - (\Gamma_2)_{SV}$ vs. X_2 for polymethylmethacrylate.

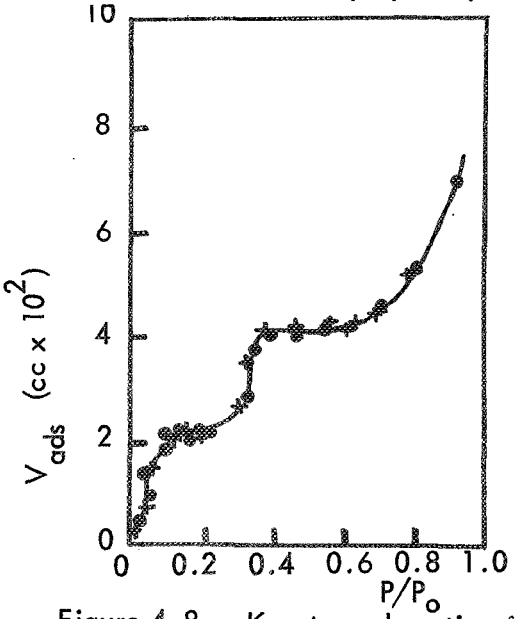

Figure 4.8. Krypton adsorption isotherm for polymethylmethacrylate at 78 K

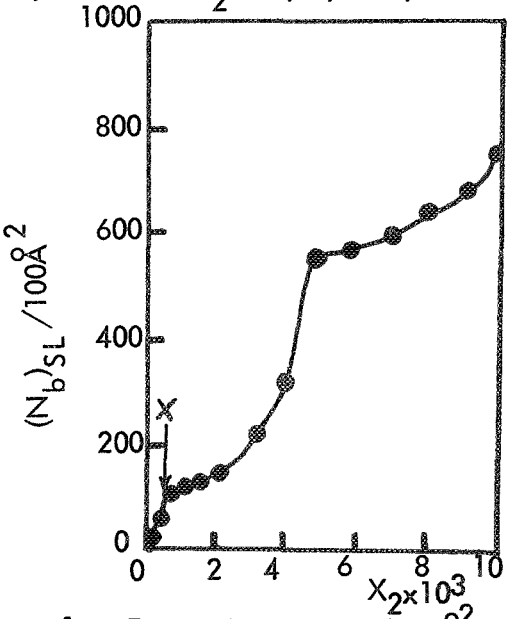

Figure 4.9. N_b /100Å^2 vs X_2 for butanol adsorbed on polymethylacrylate.

The situation is less clearcut than with polystyrene for two reasons. Firstly, the surface area of the polymethylmethacrylate poder (figure 4.8) was lower than that of polystyrene (about $0.12\ m^2g^{-1}$ compared with $1.5\ m^2g^{-1}$). Secondly, a two-step isotherm was obtained for the adsorption of krypton at 78°K (see figure 4.8.) This must be attributed to a phenomenon such as capillary condensation[9] occurring at low P/p_o values ($P/p_o \simeq 0.3$) compared with $P/P_o \rightarrow 1$ for multilayer formation. This could be due to the formation of microcracks during the grinding procedure. Figure 4.9 is constructed using the value of the area given above calculated using the first knee of the isotherm; even if the second knee were used in this calculation, the first point of inflexion in figure 4.9 corresponds to mutilayer formation. Point X again corresponds to the onset of the straight line section (Point C) in figure 4.6, and this occurs at much lower concentrations than with polystyrene. Hence, of a monolayer section occurs such as observed with polystyrene (figure 4.4), it does so at very low concentrations, and would not be detected by either contact angle measurement or gas chromatography. Figure 4.10 shows the isotherm calculated as for the adsorption at the solid-vapour interface. This is essentially the same as for the solid-liquid interface, and so the nature of the adsorption at both interfaces is similar. The occurrence of multilayer formation at lower concentrations on polymethylmethacrylate may indicate that butanol is more strongly adsorbed on this polymer than on polystyrene.

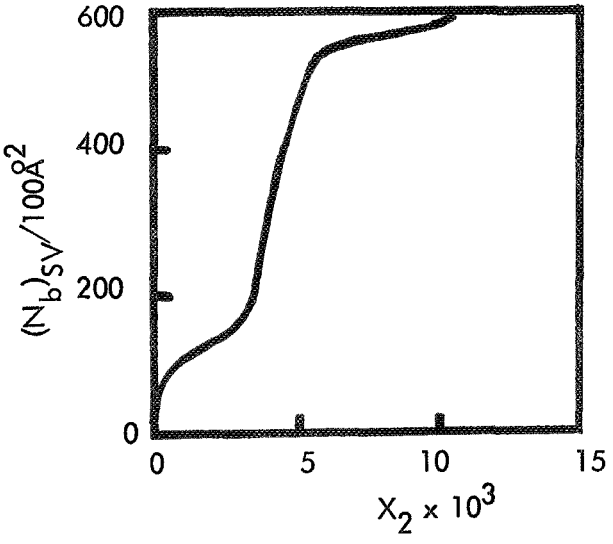

Figure 4.10. Calculated butanol adsorption isotherm for the solid-vapour interface.

We can now use the results for the two systems to draw conclusions about the nature of the surfaces obtained by the polymerisation of perfluorobutene-2 on a tungsten substrate using the electron beam polymerisation technique.

4.3.2. Polyperfluorobutene-2.

4.3.2.1. Results of Contact Angle Measurements.

Table 4.1 summarises the types of experiments conducted to date. Repeat experiments have shown that the results are completely reproducible over several separate samples of each type of polymer. The standard conditions of preparation are taken to correspond to a grid voltage (see reference 1 for gun geometry) of 35V, an anode voltage of 500V, a filament current of 1.3A and a flux rate of x1. The flux rate is an arbitrary quantity, corresponding to a fixed monomer reservoir pressure and corresponding to a dynamic partial pressure of perfluorobutene-2 in the reaction vessel of about 5×10^{-5} torr. Conditions shown in brackets in table 4.1 indicate that these are also part of other series shown earlier in the table. The table also shows the numbers of the figures in which the contact angle data for each series is plotted. In each of figures 4.11 to 4.17, (a) is a plot of $\cos\theta$ vs γ_{LV} and (b) is a plot of $\{(\Gamma_2)_{SL} - (\Gamma_2)_{SV}\}$ vs activity. In several of the experiments shown, the limits of possible error in the values of $\{(\Gamma_2)_{SL} - (\Gamma_2)_{SV}\}$ are indicated by vertical lines. This shows that the trends in these composite isotherms are completely meaningful.

4.3.2.2. Discussion of Contact Angle Results for Polyperfluorobutene-2.

The experiments shown in table 3.1 were designed to show how the surface adsorption properties changed when all but one variable was kept constant during the preparation of the polymers. It is possible to separate each isotherm in a qualitative way to give curves similar to those shown in figures 4.4 and 4.5 or 4.9 and 4.10. When there is a maximum or minimum at low concentration, we have evidence for a two-step isotherm, and when the isotherm falls below the concentration axis, the adsorption at the solid-vapour interface at that concentration is more extensive than at the solid-liquid interface.

TABLE 4.1.

Series	Variable	Grid Voltage	Anode Voltage	Filament Current	Flux Rate	Substrate Temperature	Figure Number
1	Anode voltage	35V	300V	1.3A	x 1	25°C	4.11
		"	500V	"	"	"	"
		"	1000V	"	"	"	"
		"	2000V	"	"	"	"
		"	3000V	"	"	"	"
2(a)	Grid voltage	(35V	300V	1.3A	x 1	25°C)	4.12
		100V	"	"	"	"	"
		300V	"	"	"	"	"
2(b)	Grid voltage	(35V	500V	1.3A	x 1	25°C)	4.13
		100V	"	"	"	"	"
		300V	"	"	"	"	"
		500V	"	"	"	"	"
2(c)	Grid Voltage	(35V	1000V	1.3A	x 1	25°C)	4.14
		100V	"	"	"	"	"
		300V	"	"	"	"	"
		500V	"	"	"	"	"
		600V	"	"	"	"	"
		700V	"	"	"	"	"
3	Filament Temperature	(35V	500V	1.3A	x 1	25°C)	4.15
		35V	"	1.5A	"	"	"
4	Flux Rate	(35V	500V	1.3A	x 1	25°C)	4.16
		"	"	"	x 5	"	"
		"	"	"	x 10	"	"
		"	"	"	x 20	"	"
5	Substrate Temperature	(35V	500V	1.3A	x 1	25°C)	4.17
		"	"	"	"	-195°C	"

Two series of results will be discussed first, namely where the voltage of the grid (series 1) or anode (series 2a) was varied. The composite isotherms in figures 4.11 and 4.12 show two distinct trends. When the grid voltage is kept constant (and low) and the anode voltage is varied (figure 4.11) there appears to be little difference in the position of the minimum at low concentration, but there is a considerable change in the position of the subsequent maximum. Conversely, in figure 4.12, it is seen that when the anode voltage is kept constant and V_G is varied, the minimum disappears almost completely as V_G is increased, whereas the maximum is almost the same for all three grid voltages. Previous work[1] has indicated that an increase in grid voltage will increase the negative ion current, as the field at the filament is controlled by the grid. Conversely, the voltage on the anode will control only the energy of the incident ions and electrons (until the value of V_A is so high that it controls the field at the filament rather than V_G). Thus, a change in the minimum (figure 4.12) may reflect a change in the number of ions formed, and hence ultimately the thickness of the polymer. Contact angle measurement using pure liquids (figure 3.9, reference (1)) showed that χ_C decreased with increase in V_G. This implies that the surface energy decreased with increasing polymer thickness, and hence it would be expected that the adsorption of butanol at low concentrations would become less specific and hence the first step of the individual isotherms would be decreased. This is reflected by a decrease in the magnitude of the minimum in figure 4.12. When the grid voltage is kept constant, the polymer thickness will remain essentially constant with constant preparation times, but its character will be altered by the energy of the bombarding particles (variation of V_A). Hence the magnitude of the second steps of the individual isotherms will be altered. Figure 4.11 (b) shows that increasing the value of V_A up to 1000V increased the extent of adsorption at the solid-vapour interface relative to the solid-liquid interface. When V_A is increased to 2000V, it is likely that this causes a change in the field at the surface, as mentioned above, because the reverse trend is npticed. Similar trends to that of figure 4.12 exist in figures 4.13 and 4.14, although in these cases, it would appear that the first and second steps of the individual isotherms are less distinct.

Increasing the temperature of the emitting filament (figure 4.15) will increase the number

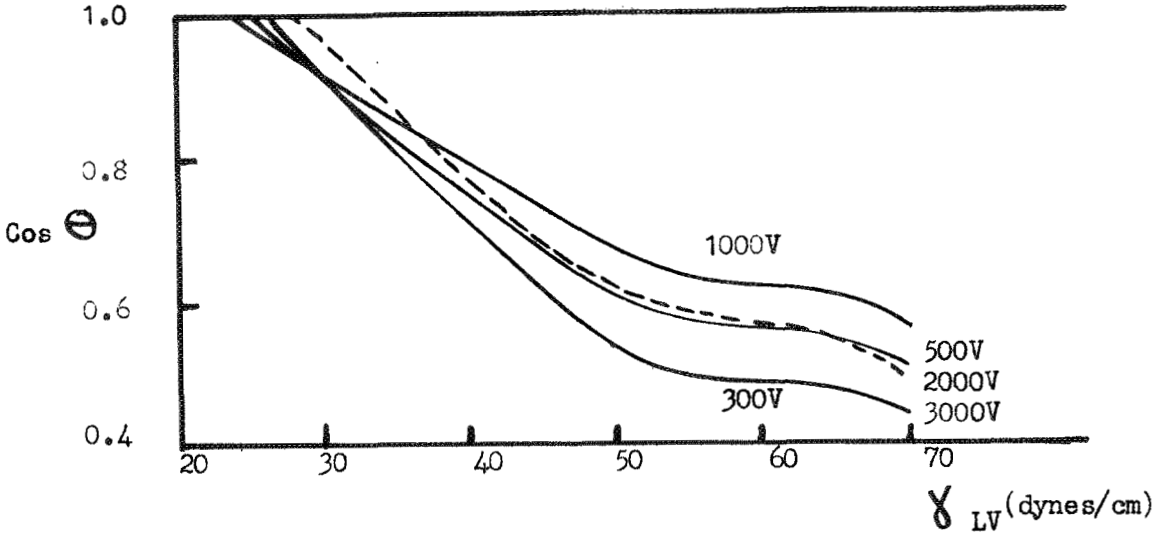

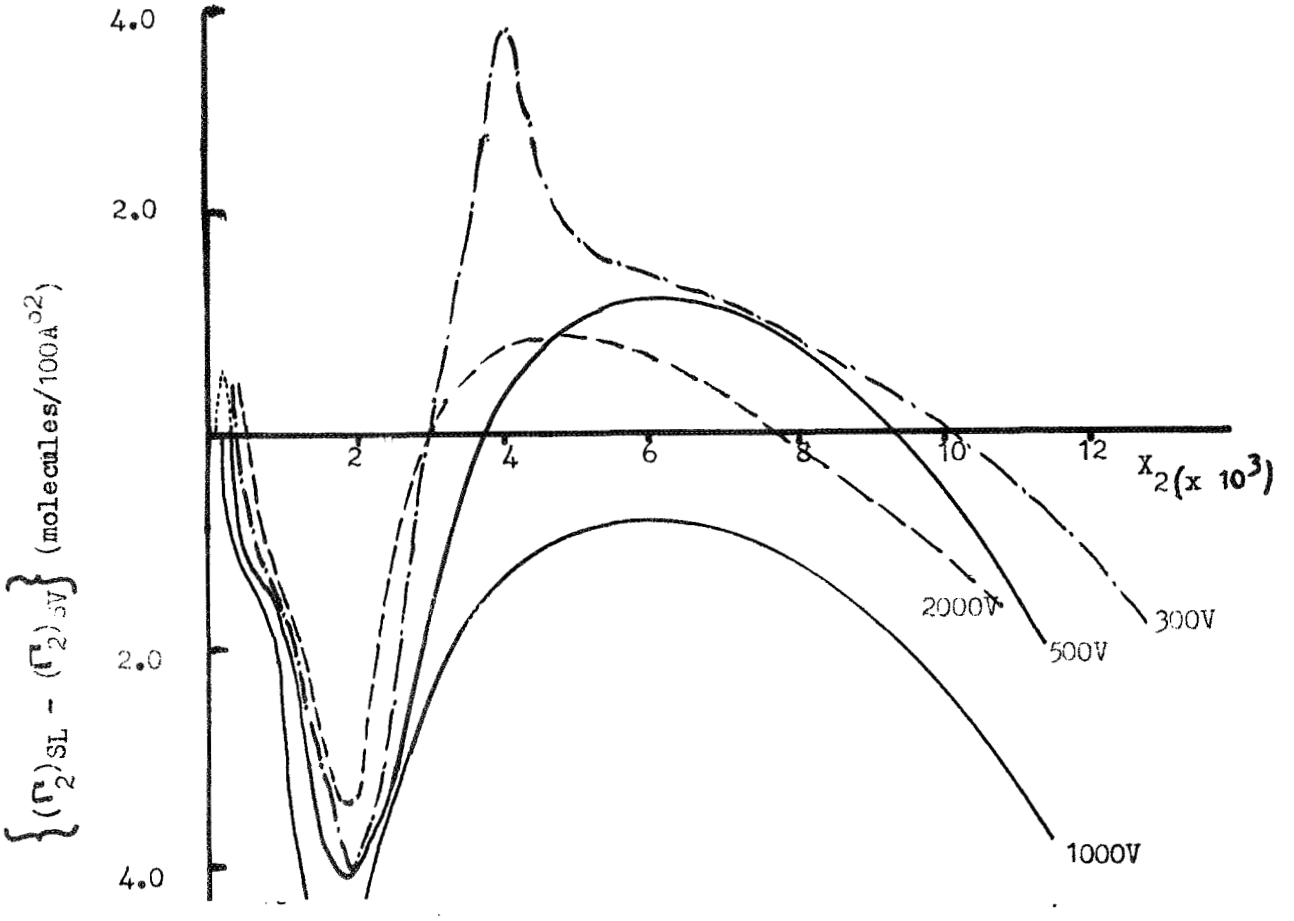

Figure 4.11. Variation of Anode Potential V_A when V_G is constant at +35V.

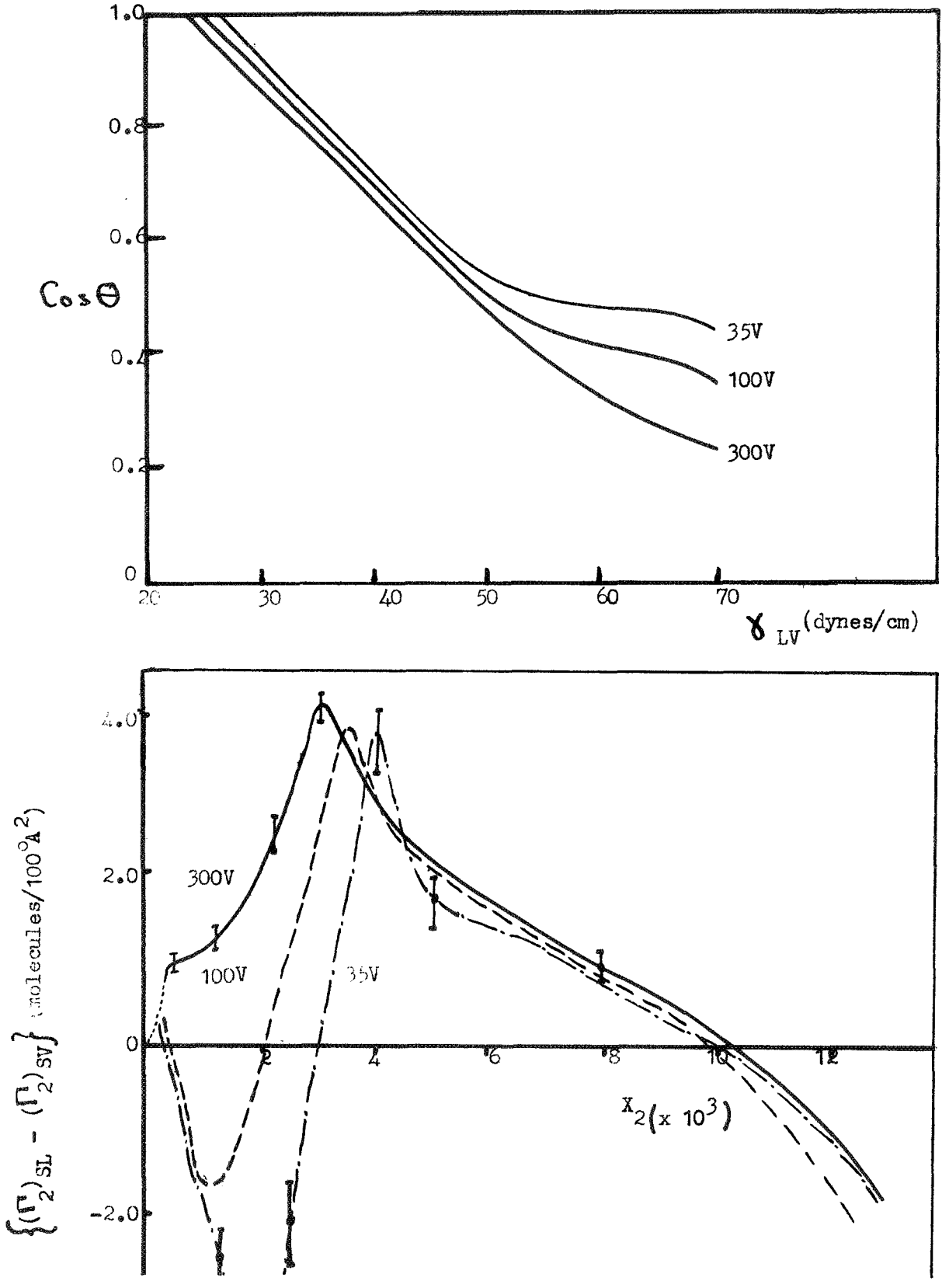

Figure 4.12. Variation of Grid Potential V_G when V_A is constant at +300V.

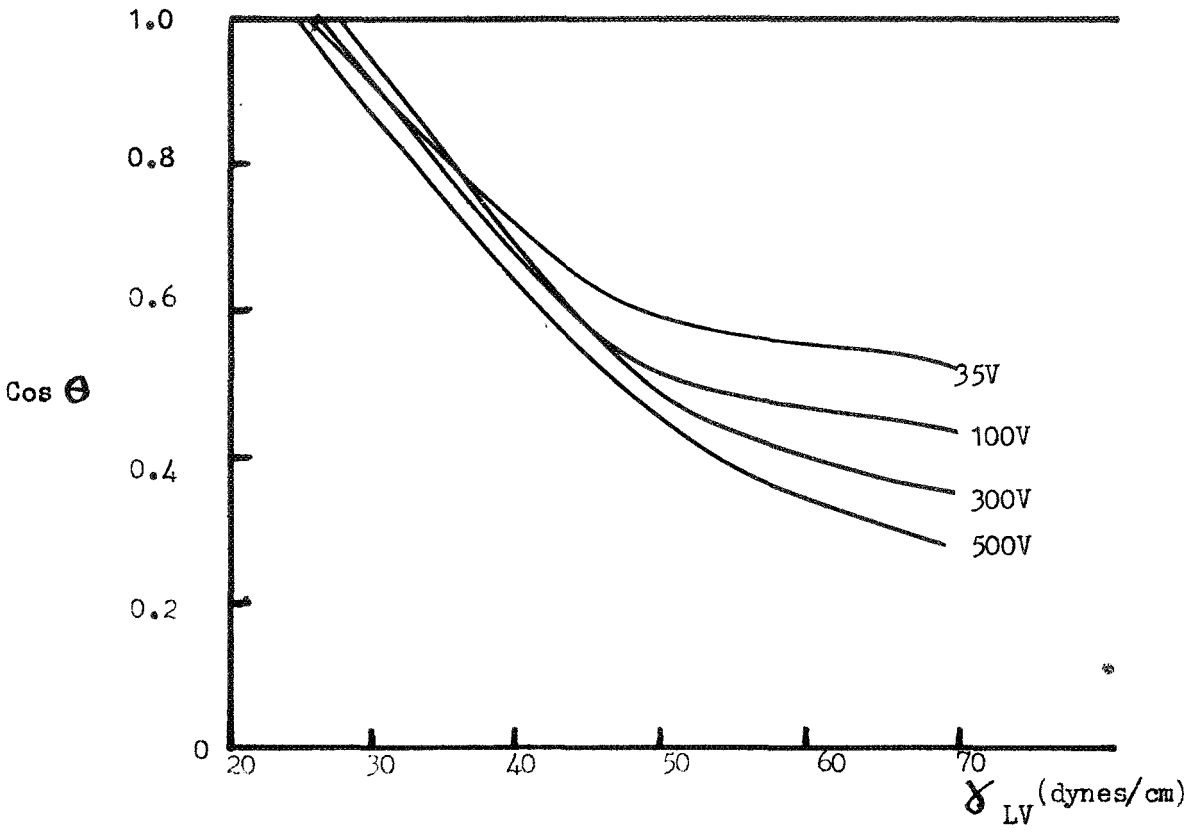

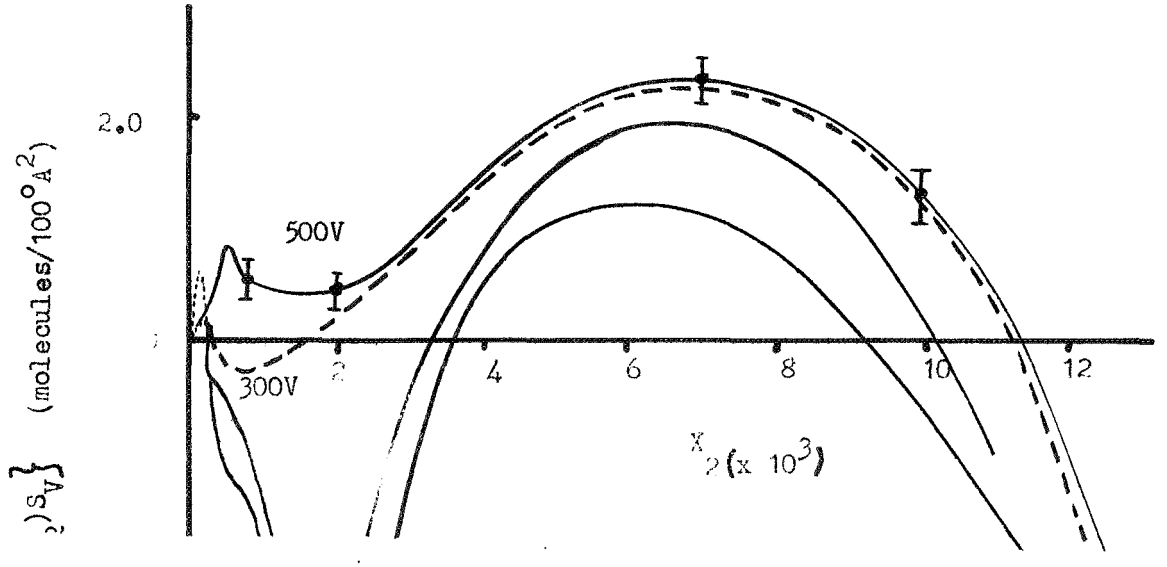

Figure 4.13. Variation of Grid Potential V_G when V_A is constant at +500V.

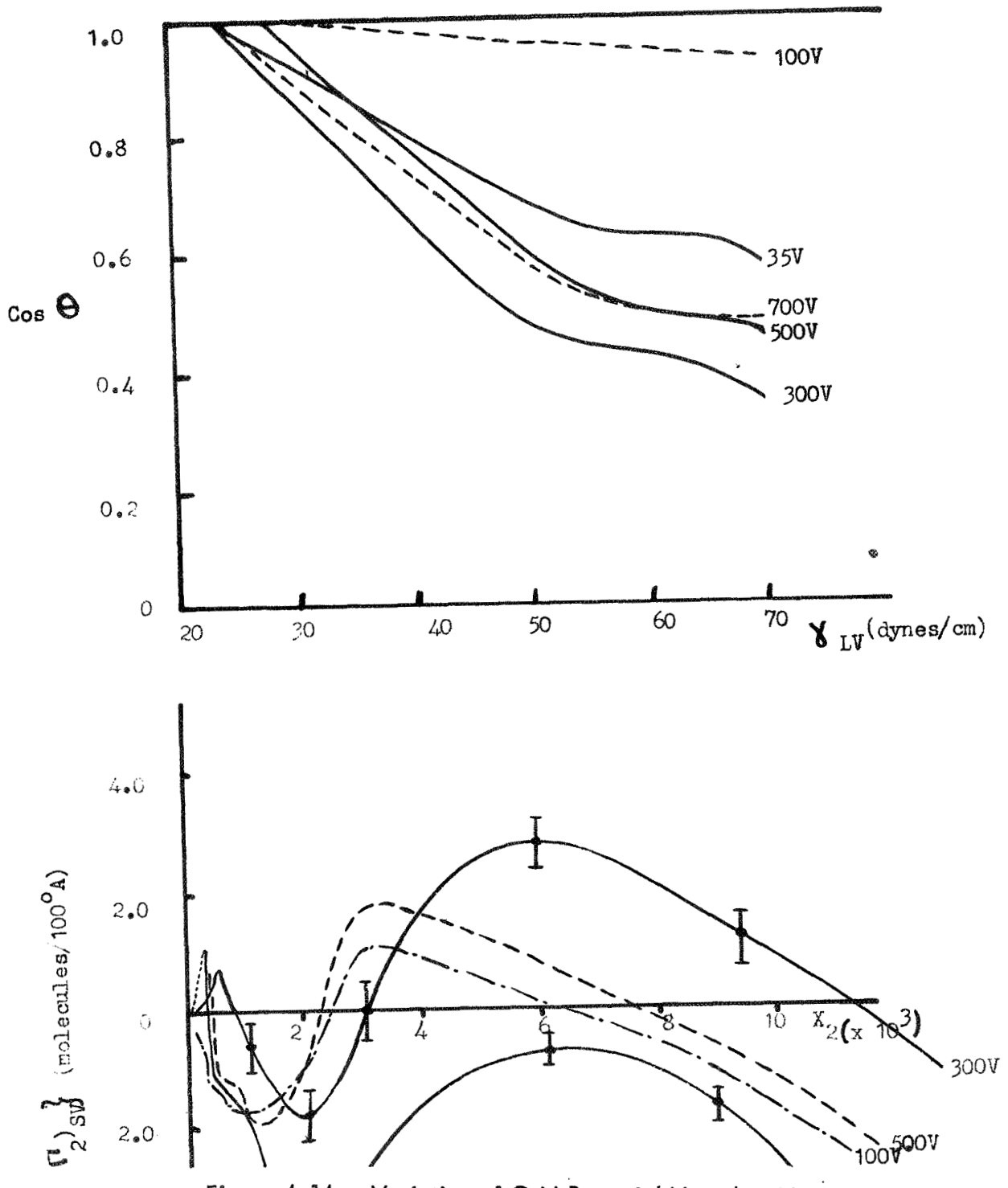

Figure 4.14. Variation of Grid Potential V_G when V_A is constant at +1000V.

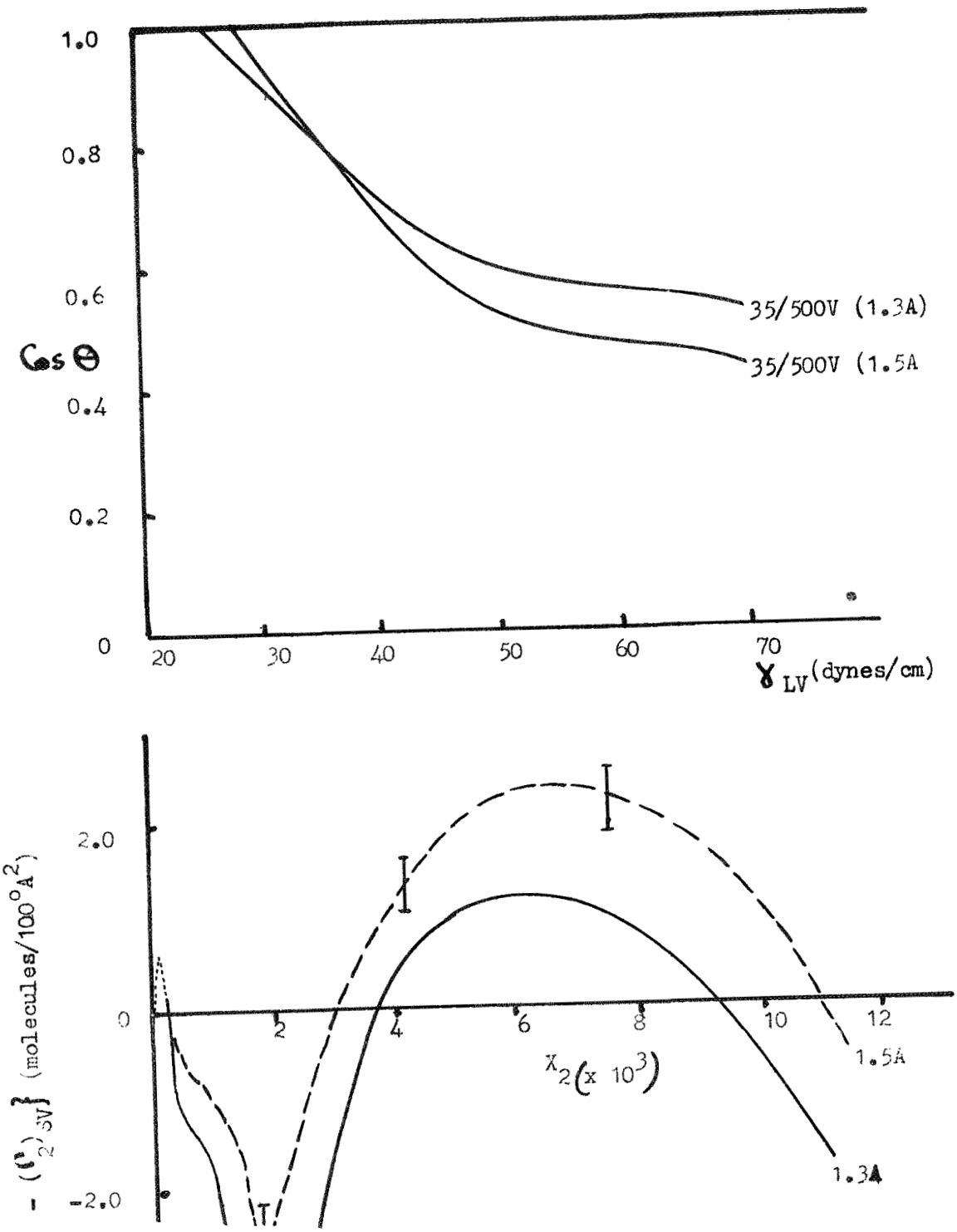

Figure 4.15. Variation of filament temperature.

of emitted electrons and ions, whereas an increase in flux rate (or monomer partial pressure) will increase the negative ion current and decrease the electron current[1]. In figure 4.15, the first minimum is decreased and the subsequent maximum is increased by an increase in filament current. If the only effect were to increase the polymer thickness, the minimum would have been expected to decrease in magnitude (see figure 4.12) as observed, but the maximum would be expected to remain constant. If the larger number of electrons formed caused greater crosslinking, then the maximum would be expected to decrease (see figure 4.11b), which is the opposite of the trend observed. Therefore, one must conclude that the increase in the maximum is due to some further variable in the process, perhaps greater breakdown of the monomer during the formation of a negative ion. The data for flux rate at a constant filament temperature (figure 4.16)

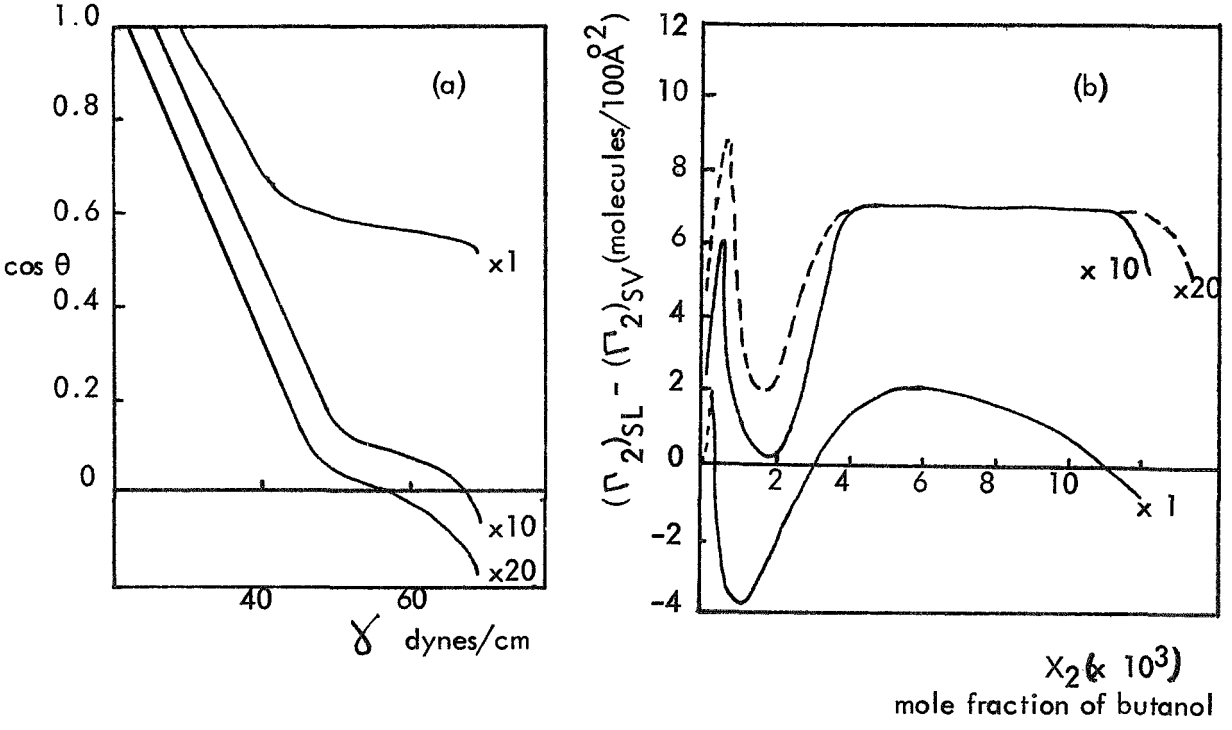

Figure 4.16. Variation of flux rate.

agree with these conclusions. Increased ion current will give increased polymer thickness; a decrease in the minimum and an increase in the first maximum are observed. Fewer electrons will be formed and therefore less crosslinking will occur and the second maximum will increase, as observed. As the second maximum reaches a limiting value,

it would appear that these conditions might relate to the minimum cross-linking possible, at least at the filament temperature used.

When the substrate is maintained at a temperature of 78K, the polymerisation process must occur entirely at the substrate. The monomer will be condensed on the surface with a relatively low partial pressure in the gas phase, and hence collisions with the filament surface will be negligible. When reaction using tetramethylsilane as monomer

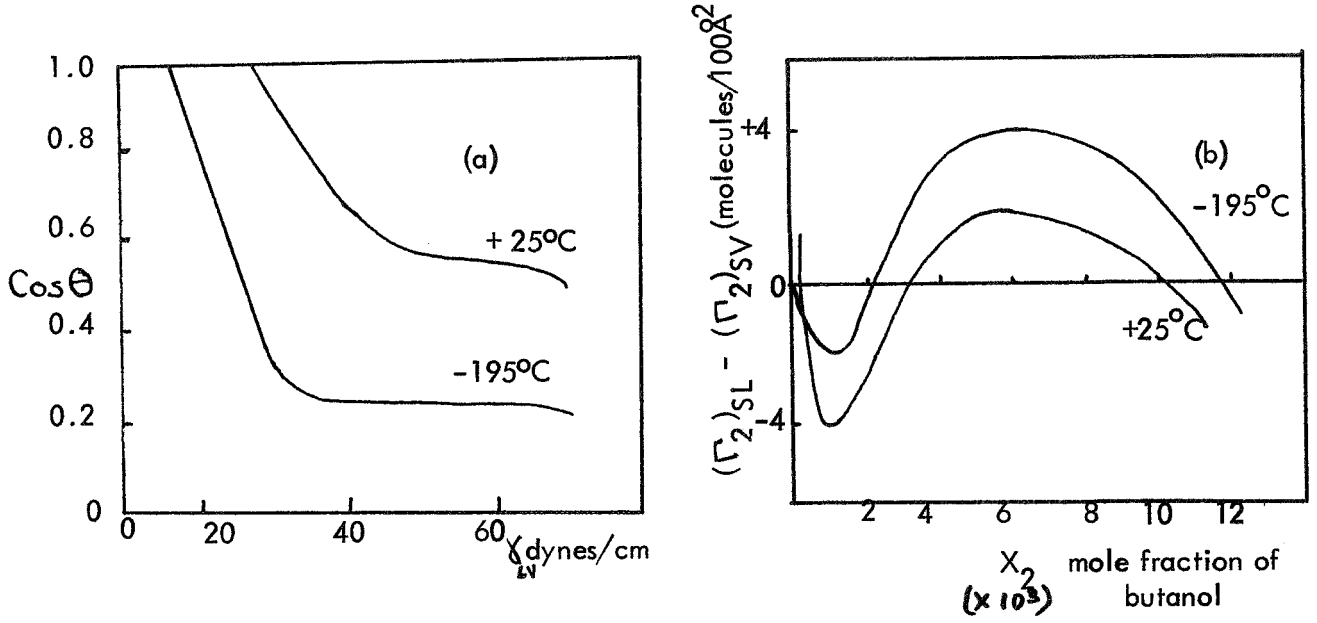

Figure 4.17. Variation of substrate temperature.

is carried out with these conditions, the stoichiometry of the reaction is very different to that in which negative ions are formed.[10] Less cross-linking of the polymer was inferred. In the same way, the contact angle data for films of polyperfluorobutene-2 prepared in the two ways are very different (figure 4.17). No initial maximum is observed and the minimum decreases and the second maximum decreases. This is consistent with much less cross-linking, as inferred with tetramethylsilane.[10]

Several of these conclusions are of necessity rather vague, because the number of possible variables in the system is large, even when only one parameter is varied at a time. However, the results do demonstrate in an unambiguous fashion that all the parameters associated with the formation of negative ions have a marked effect on

the properties of the resultant polymer. This would not be the case if free radical reactions at the filament, in the gas phase, or on the substrate were the rate determining step. Hence, these results are strong evidence for the mechanism of the polymerisation reaction proposed in this and earlier reports.

4.3.3. Film Thickness Measurements.

Film thickness measurements have been made on a series of polyperfluorobutene-2 samples. Thin films of tungsten were formed as usual and then half the film was masked off and polymer was formed on the other half. The step height was measured using the "air wedge" interference method; figure 4.18 illustrates schematically the apparatus used. Monochromatic sodium light was used. Film thicknesses were measured as a function of time of preparation and substrate temperature. A typical interference pattern is shown in figure 4.19, and typical results are shown in figure 4.20. It is seen that a

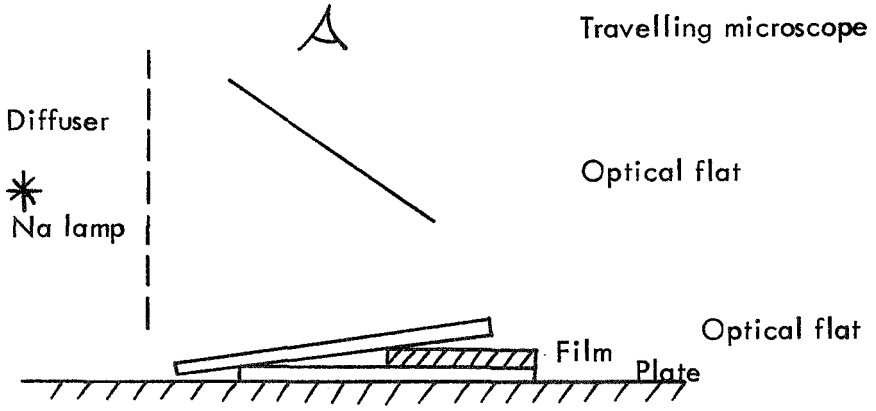

Figure 4.18 Schematic "Air Wedge" Interference Apparatus

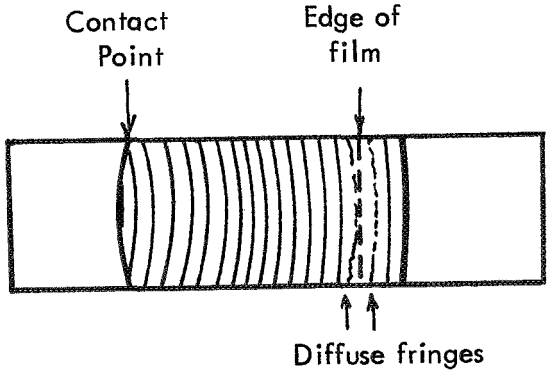

Figure 4.19 Schematic view of typical interference pattern.

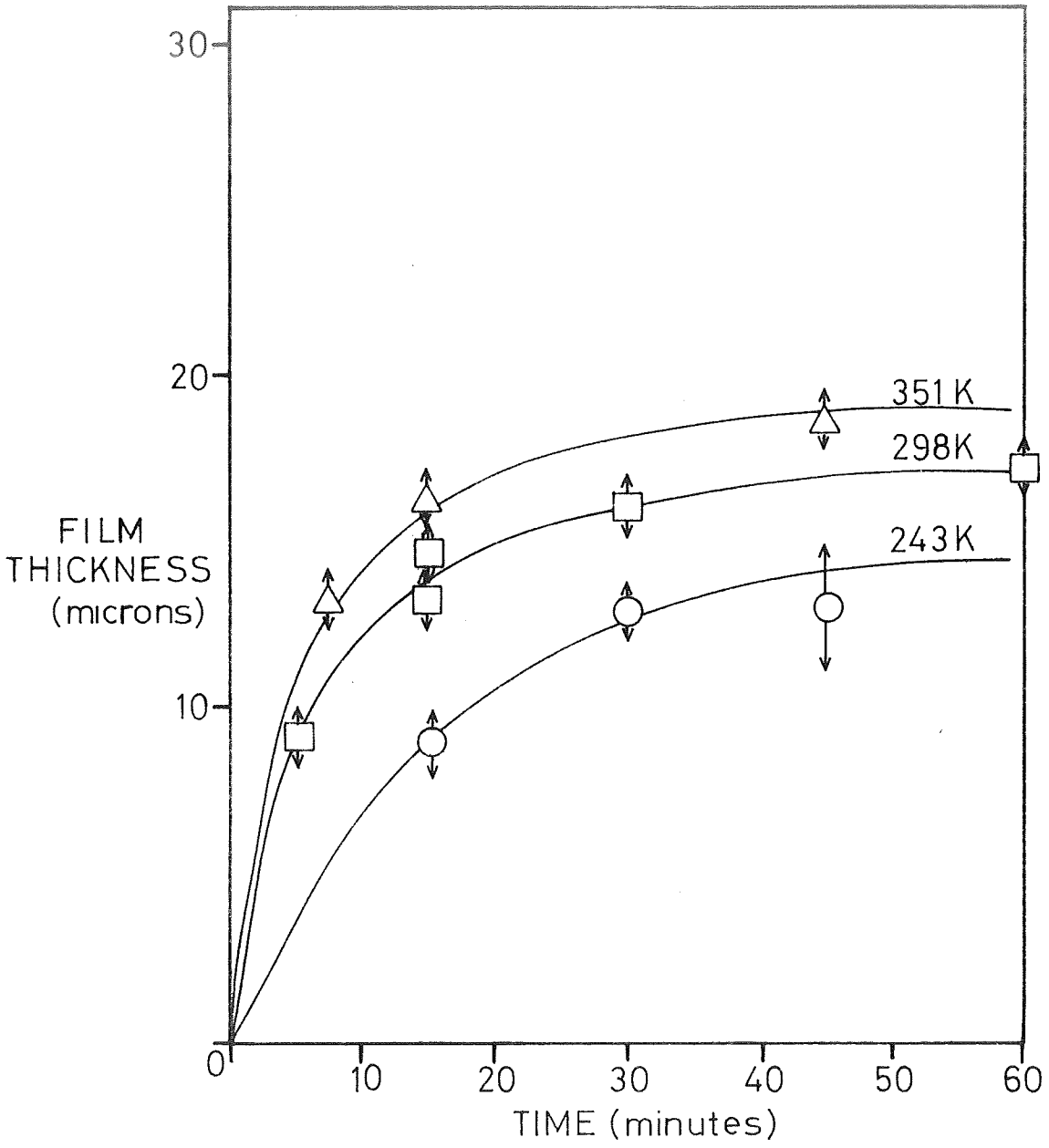

Figure 4.20

thicker film is formed with higher substrate temperatures; also, the growth of the film is not linear with time. Hence, it would appear that the polymerisation at the anode is an activated process which depends on film thickness, i.e. it becomes less probable as the polymer builds up. This may be due to negative ions being neitralised and desorbed at neutral species rather than being incorporated in the film once an appreciable film has formed. This conclusion is strengthened by the data showing a change in surface

properties of the completed polymer as a function of preparation time given above. These results emphasise the need to examine the reaction of negative ions on striking the anode.

4.4. GENERAL CONCLUSIONS.

Thin films of perfluorobutene-2 have been prepared by the electron bombardment technique under a large variety of conditions. They are uniform in thickness and are unreactive towards common organic solvents and inorganic acids, apparently providing a protective coating for the metal substrate. They are adherent to the substrate, the polymer apparently being as strongly bonded to the substrate as the metal substrate is to the underlying glass plate.

The surface properties of the resultant polymer are very dependent on the preparation conditions, as shown by contact angle measurements using butanol solutions. It is probable that frictional and anticoldwelding properties will be similarly affected, and are probably worth further study. Considerable interest is also centered on the adhesion of the polymers to the substrate and this therefore warrants a more quantitative examination. The theory of the contact angle measurement using solutions has been established unambiguously for several bulk polymers and applied qualitatively to the thin films, and trends in the surface properties are discussed. The results provide very strong support for the mechanism of the polymerisation process proposed earlier.[1]

REFERENCES.

1. M. W. Roberts, J. R. H Ross, J. H. Wood and W. J. Murphy. Final report to T.R.W. Systems, October 1969.

2. F. M. Fowkes and W. D Harkins, J. Amer. Chem. Soc., 62, 3377, (1940).

3. M. W. Roberts, Quarterly Reports to T.R.W. Systems, January - March, 1970.

4. W. A. Zisman, Advances in Chemistry Series, 43, 1, (1964) (Amer. Chem. Soc.)

5. J. W Whalen, J. Colloid and Interface Sci., 28, 443, (1968).

6. M. K. Bernett and W. A. Zisman, J. Chem. Phys., 63, 1241, (1959).

7. M. Litt and J. Herz, J. Coll. and Interface Sci., 31, 248, (1969).

8. M. K. Bernett and W. A. Zisman, J. Chem. Phys., 63, 1911, (1959).

9. See, for example, D. M. Young and A. D. Crowell, "Physical Adsorption of Gases", Butterworths, (London), 1962.

10. M. W. Roberts and J. R. H. Ross, Final Report to T.R.W. Systems, 1967.

5.0. CONCLUSIONS AND RECOMMENDATIONS.

5.1. CONCLUSIONS.

5.1.1. Carburisation of tungsten.

The results of a study of the carburisation of tungsten by a series of hydrocarbons have been presented. The effective work function for thermionic emission ($\emptyset^{**}$) of the carburised surface was about 2.5 eV, but the average work function ($\overline{\emptyset}$) was 5.05 eV.

5.1.2. Use of rhenium as a filament material.

Rhenium, contrary to expectation, appears to form a carbide or carbides. After the carburisation reaction is complete, the filament has a constant apparent work function, and can therefore be used in kinetic studies of the polymerisation reaction.

5.1.3. Surface studies of thin polymeric films.

The use of contact angle measurements for studying the surface properties of polymers has been examined in detail and the variation of the properties of the polymer formed from perfluorobutene-2 under various conditions has been examined. The polymers are transparent, relatively chemically inert, and adherent to the underlying metal substrate. The wetting results are consistent with the mechanism already suggested for the polymerisation process (see Part 1).

5.2. RECOMMENDATIONS.

5.2.1. Kinetics of Polymerisation.

The carbide of rhenium should be used as an emitting filament in the study of the kinetics of the polymerisation reaction, with particular reference to the effect of an applied field. This work would have considerable theoretical relevance as well as being of practical importance in the prediction of of the best monomer/emitter combination for thin film formation.

5.2.4. Identification of Negative Ions .

The nature of the negative ions in the polymerisation process should be ascertained; this programme would involve the development of a negative ion mass-spectrometer (see section 6.1) using the emitting filament as a source of ions.

5.2.5. Polymer properties.

The mechanical and chemical properties of the carbide of rhenium should be examined.

5.2.6. New materials.

The wetting study should be extended to a survey of other monomer/substrate combinations, with particular reference to a search for low energy surfaces with low chemical reactivity.

5.2.7. Extension of Study to Thicker Films.

The wetting studies should be related to the physical and chemical properties of the polymer, and the polymer/substrate adhesion characteristics. Of particular interest would be the preparation of thicker films and the development of more quantitative testing methods for examining the properties of these films; the results could then be extrapolated to thin films. In particular, the chemical structure of the films might be examined, and the dependence of adhesion on substrate/monomer interaction could be investigated quantitatively.

6.0. NEW TECHNOLOGY.

6.1. NEGATIVE ION MASS SPECTROMETER.

The high efficiency of the formation of negative ions at an electron emitting filament suggests the possibility of using a suitably stabilised emitter as a source for a mass spectrometer operating with negative rather than positive ions. The source could be used with conventional mass analysers (magnetic analysers, quadrupole filters, etc.) and detectors (see figure 6.1.)

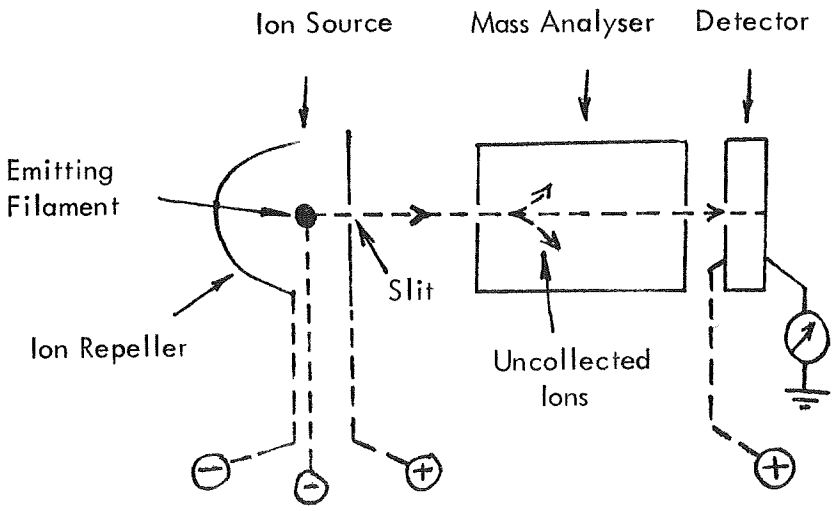

Figure 6.1.

Negative Ion Mass Spectrometer

Such a source would have the following advantages:-

(a) robust and very compact, with simple construction,

(b) require simple electronic control,

(c) capability of operation at relatively high pressures ($\sim 10^{-2}$ torr),

(d) considerably higher sensitivity than conventional sources of positive ions. At suitable emitter temperatures, the efficiency of the reaction is unity i.e. one ion is produced for every molecule striking the filament. If the filament area is ~ 0.1 cm^2, $\sim 5 \times 10^{16}$ ions will be formed per second at 10^{-3} torr, which corresponds to a current of $\sim 5 \times 10^{-3}$ amp, or a sensitivity of 5 amp torr^{-1}. This should be compared with the sensitivity of a conventional positive ion spectrometer of $\sim 10^{-5}$ amp torr^{-1}.

(e) By choice of suitable filament material for any desired application, effects of contamination by background gases, such as H_2O, H_2S. etc. can be minimised.

Together with a suitable analyser of short path length of the types currently being developed, the source would enable low partial pressures of contaminant gases to be detected; such an arrangement would be small and could be pumped solely using a mechanical pump, enabling its use in situations when compactness is advantageous. The following possible uses are suggested:-

(a) detection of OF_2,

(b) detection of CO in exhaust fumes,

(c) detection of SO_2 in smoke,

(d) oxygen partial pressure measurement.

6.2. LOW WORK FUNCTION EMITTER.

Under certain conditions, tungsten gives a low work function emitter in the presence of hydrocarbons (p.2 - 12).

6.3. RHENIUM CARBIDE .

It has been shown that rhenium carbide may be formed from the reaction of rhenium with hydrocarbons (p.3 - 8). Rhenium itself is a useful high temperature material and its carbide might have even more suitable properties. A carbide of rhenium has never been positively[1] identified.

6.4. NEGATIVE TEMPERATURE COEFFICIENT OF ELECTRON EMISSION.

A previously unreported phenomenon has been noted, namely, rhenium carbide has an apparent negative work function over certain ranges of temperature and carbide composition (p.3 - 7). Effectively, the emission current from a filament decreases as the filament temperature is increased; this might find an application in electronics.

6.5. POLYMERIC COATING WITH CONTROLLABLY VARIABLE SURFACE ENERGY.

Thin polymeric films prepared by the electron bombardment technique have been shown to have surface properties, e.g. surface energy, dependent on the preparation conditions such as electron gun potentials, substrate temperature, etc. (see pp. 4-10 to 4-20). The surface energies may range from very low (comparable with the surface energy of bulk teflon) to relatively high values. The films are in all cases strongly adherent to the substrate (p.4-21), and provide protection from common solvents (see ref.2, p.A-13). The films may have a variety of applications, such as:-

(a) Inert polymeric coatings for fuel chambers,

(b) Mechanically stable valve seatings,

(c) Lubricants and anticoldwelding coatings,

(d) Selective adsorbents,

(e) Coatings for artificial heart components, to prevent blood cell damage,

(f) Coatings for glass-fibre or carbon-fibre filaments used in reinforced materials; these intermediate coatings might be developed to increase the adhesion of one material to the other.

6.6. ADSORPTION BY LOW ENERGY SOLIDS OF SURFACE ACTIVE AGENTS.

The adsorption of surface active agents on low energy solids (see p. 4-1) has not been recognised as a general phenomenon although one such situation has previously been reported[3]. This has many repercussions in colloid and surfactant chemistry, for example:-

(a) detergency,

(b) ore flotation,

(c) emulsion polymerisation,

(d) electrokinetic phenomena,

(e) dyeing.

The realisation that surfactants are adsorbed could lead to new classes of surfactants which would remain adsorbed after the solution was removed and which would serve

as protective coatings, e.g. on fabrics. Alternatively it is suggested that surfactants could be developed which, when added to corrosive liquids, would form a barrier between the liquid and the container as long as the liquid was present.

REFERENCES.

1. "Constitution of Binary Alloys" 2nd Supplement, edited by F. A. Shunk, McGraw Hill, N.Y., 1969.

2. M. W. Roberts, J. R. H. Ross and J. H. Wood, in Vol.1 of Advanced Valve Technology Report, January 1969, Contract NAS7-436.

3. M. K. Bernett and W. A. Zisman, J. Chem. Phys., 63, 1911, (1959)